Supporting Information for

Heterogeneous Heck Coupling in Multivariate Metal-Organic Frameworks for Enhanced Selectivity

Jonathan W. Brown,[a] Nanette N. Jarenwattananon,[a] Trenton Otto,[a] James L. Wang,[a] Stefan Glöggler,[a] Louis-S. Bouchard,[a,*]

[a] Department of Chemistry and Biochemistry, University of California, Los Angeles, California 90095, United States

* To whom correspondence should be addressed: louis.bouchard@gmail.com (L.-S.B)

Section S1: Materials and general procedures

All reagents, unless otherwise stated, were obtained from commercial sources (Alfa Aesar, Cambridge isotope laboratories, Sigma Aldrich, TCI) and were used without further purification. Reported MOF crystallization yields were unoptimized. All experiments other than ICP-AES (performed at University of Southern California) were performed at the University of California, Los Angeles, Department of Chemistry and Biochemistry.

Section S2: Synthesis of all $Zn_4O(BDC\text{-}NH_2)_n(BDC)_{(3-n)}$ (n = 3, 2.4, 1.8, 1.2, 0.9, 0.75, 0.6, 0.3, and 0.15) samples

$Zn_4O(C_8H_4O_4)_{2.85}(C_8NH_5O_4)_{0.15}$. A mixture of 2-Aminoterephthalic acid ($H_2BDC\text{-}NH_2$) (9 mg, 0.05 mmol), benzenedicarboxylic acid (H_2BDC) (157 mg, 0.950 mmol) and zinc nitrate hexahydrate (890 mg, 3.0 mmol) was added to *N*,*N*-dimethylformamide (DMF) (50 mL) and sonicated until the components were fully dissolved. The static solution was heated at 85 °C for 24 h to form single crystals. The crystals were collected and washed with DMF (3 × 30 mL) over a 3-h period.

$Zn_4O(C_8H_4O_4)_{2.7}(C_8NH_5O_4)_{0.3}$. A mixture of 2-Aminoterephthalic acid ($H_2BDC\text{-}NH_2$) (18 mg, 0.10 mmol), benzenedicarboxylic acid (H_2BDC) (149 mg, 0.90 mmol) and zinc nitrate hexahydrate (890 mg, 3.0 mmol) was added to *N*,*N*-dimethylformamide (DMF) (50 mL) and sonicated until the components were fully dissolved. The static solution was heated at 85 °C for 24 h to form single crystals. The crystals were collected and washed with DMF (3 × 30 mL) over a 3-h period.

$Zn_4O(C_8H_4O_4)_{2.4}(C_8NH_5O_4)_{0.6}$. A mixture of 2-Aminoterephthalic acid ($H_2BDC\text{-}NH_2$) (63 mg, 0.34 mmol), benzenedicarboxylic acid (H_2BDC) (108 mg, 0.650 mmol) and zinc nitrate hexahydrate (890 mg, 3.0 mmol) was added to *N*,*N*-dimethylformamide (DMF) (50 mL) and sonicated until the components were fully dissolved. The static solution was

heated at 85 °C for 24 h to form single crystals. The crystals were collected and washed with DMF (3 × 30 mL) over a 3-h period.

$Zn_4O(C_8H_4O_4)_{2.25}(C_8NH_5O_4)_{0.75}$. A mixture of 2-Aminoterephthalic acid ($H_2BDC\text{-}NH_2$) (45 mg, 0.25 mmol), benzenedicarboxylic acid (H_2BDC) (124 mg, 0.750 mmol) and zinc nitrate hexahydrate (890 mg, 3.0 mmol) was added to *N*,*N*-dimethylformamide (DMF) (50 mL) and sonicated until the components were fully dissolved. The static solution was heated at 85 °C for 24 h to form single crystals. The crystals were collected and washed with DMF (3 × 30 mL) over a 3-h period.

$Zn_4O(C_8H_4O_4)_{2.1}(C_8NH_5O_4)_{0.9}$. A mixture of 2-Aminoterephthalic acid ($H_2BDC\text{-}NH_2$) (54 mg, 0.3 mmol), benzenedicarboxylic acid (H_2BDC) (116 mg, 0.70 mmol) and zinc nitrate hexahydrate (890 mg, 3.0 mmol) was added to *N*,*N*-dimethylformamide (DMF) (50 mL) and sonicated until the components were fully dissolved. The static solution was heated at 85 °C for 24 h to form single crystals. The crystals were collected and washed with DMF (3 × 30 mL) over a 3-h period.

$Zn_4O(C_8H_4O_4)_{1.8}(C_8NH_5O_4)_{1.2}$. A mixture of $H_2BDC\text{-}NH_2$ (120 mg, 0.66 mmol), H_2BDC (100 mg, 0.60 mmol) and zinc nitrate hexahydrate (890 mg, 3.0 mmol) was added to DMF (50 mL) and sonicated until the components were fully dissolved. The static solution was heated at 85 °C for 24 h to form single crystals. The crystals were collected and washed with DMF (3 × 30 mL) over a 3-h period.

$Zn_4O(C_8H_4O_4)_{1.2}(C_8NH_5O_4)_{1.8}$. $H_2BDC\text{-}NH_2$ (136 mg, 0.750 mmol), H_2BDC (42 mg, 0.25 mmol) and zinc nitrate hexahydrate (890 mg, 3.0 mmol) was added to DMF (50 mL) and sonicated until the components were fully dissolved. The static solution was heated at 85 °C for 24 h to form single crystals. The crystals were collected and washed with DMF (3 × 30 mL) over a 3-h period.

$Zn_4O(C_8H_4O_4)_{0.6}(C_8NH_5O_4)_{2.4}$. A mixture of $H_2BDC\text{-}NH_2$ (163 mg, 0.89 mmol), H_2BDC (17 mg, 0.10 mmol) and zinc nitrate hexahydrate (890 mg, 3.0 mmol) was added to DMF (50 mL) and the mixture was sonicated until the components were fully dissolved. The static solution was heated at 85 °C for 24 h to form single crystals. The crystals were collected and washed with DMF (3 × 30 mL) over a 3-h period.

$Zn_4O(BDC\text{-}NH_2)_3$. The synthesis of IRMOF-3 was analogous to those reported in the literature.[S1] $H_2BDC\text{-}NH_2$ (180 mg, 0.99 mmol) and zinc nitrate hexahydrate (890 mg, 3 mmol) were added to DMF (50 mL) and the mixture was sonicated until the components were fully dissolved. The static solution was heated at 85 °C for 24 h to form single crystals. The crystals were collected and washed with DMF (3 × 10 mL) repeatedly over a 3-h period. PXRD was used to confirm the phase purity of the as-synthesized samples (Figure S1).

Section S3: Metalation of $Zn_4O(BDC\text{-}NH_2)_n(BDC)_{(3-n)}$ (n = 2.4, 1.8, 1.2, 0.9, 0.75, 0.6, 0.3, and 0.15)

Utilizing a two-step postmodification reaction, imine condensation followed by metalation, all samples were metalated using identical synthetic conditions.[S2] For example, a freshly solvent-exchanged sample of $Zn_4O(BDC\text{-}NH_2)_n(BDC)_{(3-n)}$ was reacted with salicyclic aldehyde in toluene to form an imine bond in the framework. Before metalation could be achieved, the framework was washed to remove excess salicyclic acid. After solvent exchange with CH_2Cl_2 was completed, $PdCl_2(CH_3CN)_2$ in CH_2Cl_2 was added, and allowed to stand at room temperature. After 48 h the sample was exchanged with CH_2Cl_2 to remove excess $PdCl_2(CH_3CN)_2$. The framework was then exposed to a vacuum (30 mTorr) at 85 °C to remove all of the solvent from the pores.

Imine formation in $Zn_4O(BDC\text{-}NH_2)_3$. DMF-exchanged $Zn_4O(BDC\text{-}NH_2)_3$ (~ 100 mg) was solvent exchanged with dry toluene (5 × 20 mL) over a 2-h period. Salicyclic aldehyde (1.0 mL, 7.1 mmol) was added to $Zn_4O(BDC\text{-}NH_2)_3$ in toluene and the reaction was allowed to stand at 50 °C for 5 days. After 5 days, the sample was exchanged with

dry toluene (5 × 20 mL) to remove unreacted salicyclic aldehyde, yielding $Zn_4O(BDC\text{-}NH_2)_3$-Imine.

Metalation of $Zn_4O(BDC\text{-}NH_2)_3$. Toluene exchanged $Zn_4O(BDC\text{-}NH_2)_3$-Imine (~100 mg) was solvent exchanged with CH_2Cl_2 (1 × 20 mL) over a 2-h period. $PdCl_2(CH_3CN)_2$ (50 mg, 0.19 mmol) was dissolved in CH_2Cl_2 (40 mL) to which the $Zn_4O(BDC\text{-}NH_2)_3$-Imine was added in a minimum amount of solvent. The reaction was allowed to stand at room temperature for 2 days, at which point it was washed with CH_2Cl_2 (3 × 20 mL) over a 2-h period, followed by CH_2Cl_2 (3 × 20 mL) over a 3-day period. The solvents were removed from the pores of the framework by vacuum pumping (at 30 mTorr) for 12 h at 85 °C to yield $Zn_4O(BDC\text{-}NH_2)_3$-Pd.

Imine formation in $Zn_4O(BDC\text{-}NH_2)_n(BDC)_{(3-n)}$ (n = 2.4, 1.8, 1.2, 0.9, 0.75, 0.6, 0.3, and 0.15). DMF exchanged $Zn_4O(BDC\text{-}NH_2)_n(BDC)_{(3-n)}$ (~ 100 mg) was solvent exchanged with toluene (5 × 20 mL) over a 2-h period. Salicyclic aldehyde (1.0 mL, 7.1 mmol) was added to $Zn_4O(BDC\text{-}NH_2)_n(BDC)_{(3-n)}$ in toluene and the reaction was allowed to stand at 50 °C for 5 days. After 5 days, the sample was exchanged with fresh toluene (5 × 20 mL) to remove unreacted salicyclic aldehyde, yielding $Zn_4O(BDC\text{-}NH_2)_n(BDC)_{(3-n)}$-Imine.

Metalation of $Zn_4O(BDC\text{-}NH_2)_n(BDC)_{(3-n)}$-Imine. Toluene-exchanged $Zn_4O(BDC\text{-}NH_2)_n(BDC)_{(3-n)}$-Imine was solvent exchanged with CH_2Cl_2 (1 × 20 mL) over a 2-h period. $PdCl_2(CH_3CN)_2$ (50 mg, 0.19 mmol) was dissolved in CH_2Cl_2 (20 mL) to which the $Zn_4O(BDC\text{-}NH_2)_n(BDC)_{(3-n)}$-Imine was added in a minimum amount of solvent. The reaction was allowed to stand at room temperature for 2 days, at which point it was washed with CH_2Cl_2 (3 × 20 mL) over a 2-h period, followed by CH_2Cl_2 (3 × 20 mL) over a 3-day period. The solvents were removed from the pores of the framework by vacuum (30 mTorr) for 12 h at 85 °C to yield $Zn_4O(BDC\text{-}NH_2)_n(BDC)_{(3-n)}$-Pd.

Section S4: Powder X-ray diffraction data

The structural integrity of the unfunctionalized frameworks [$Zn_4O(BDC\text{-}NH_2)_n(BDC)_{(3-n)}$], the imine functionalized framework [$Zn_4O(BDC\text{-}NH_2)_n(BDC)_{(3-n)}$-Imine], and the Pd functionalized framework [$Zn_4O(BDC\text{-}NH_2)_n(BDC)_{(3-n)}$-Pd] ($n$ = 3, 2.4, 1.8, 1.2, 0.9, 0.75, 0.6, 0.3, and 0.15) was confirmed by PXRD.

PXRD data were collected using a Bruker D8-Discover θ-θ diffractometer, equipped with a Vantec Line detector, in reflectance Bragg-Brentano geometry employing Ni filtered Cu Kα line-focused radiation at 1600 W (40 kV, 40 mA) power. . Radiation was focused using parallel focusing Gobel mirrors. The system was also outfitted with an anti-scattering shield that prevents incident diffuse radiation from hitting the detector, in order to mitigate the normally large background signal at $2\theta < 3$. Samples were mounted on glass slides by dropping powders from a wide-blade spatula and then leveling the sample with a razor blade.

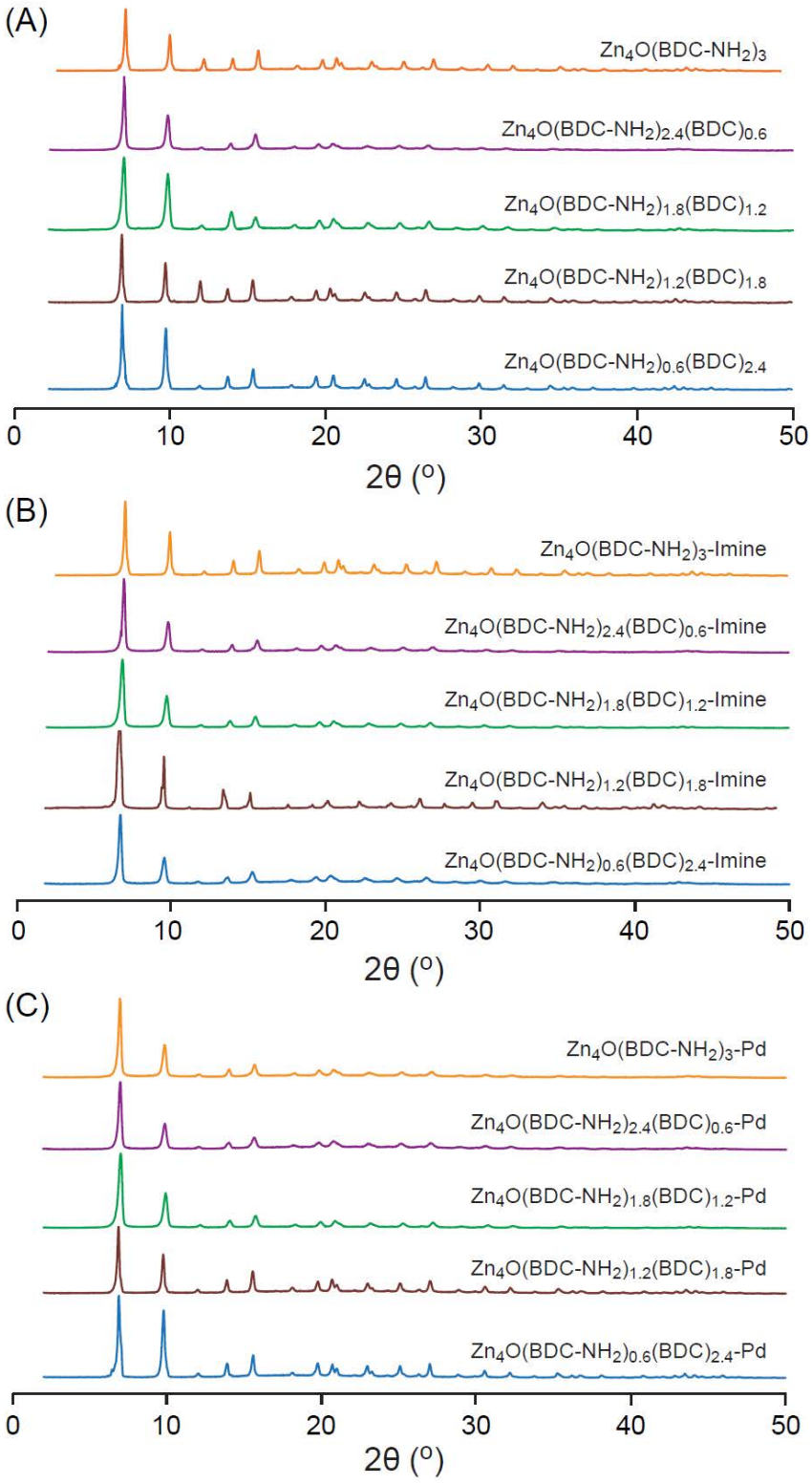
(A)
$Zn_4O(BDC\text{-}NH_2)_3$
$Zn_4O(BDC\text{-}NH_2)_{2.4}(BDC)_{0.6}$
$Zn_4O(BDC\text{-}NH_2)_{1.8}(BDC)_{1.2}$
$Zn_4O(BDC\text{-}NH_2)_{1.2}(BDC)_{1.8}$
$Zn_4O(BDC\text{-}NH_2)_{0.6}(BDC)_{2.4}$
0 10 20 30 40 50
2θ (°)
(B)
$Zn_4O(BDC\text{-}NH_2)_3$-Imine
$Zn_4O(BDC\text{-}NH_2)_{2.4}(BDC)_{0.6}$-Imine
$Zn_4O(BDC\text{-}NH_2)_{1.8}(BDC)_{1.2}$-Imine
$Zn_4O(BDC\text{-}NH_2)_{1.2}(BDC)_{1.8}$-Imine
$Zn_4O(BDC\text{-}NH_2)_{0.6}(BDC)_{2.4}$-Imine
0 10 20 30 40 50
2θ (°)
(C)
$Zn_4O(BDC\text{-}NH_2)_3$-Pd
$Zn_4O(BDC\text{-}NH_2)_{2.4}(BDC)_{0.6}$-Pd
$Zn_4O(BDC\text{-}NH_2)_{1.8}(BDC)_{1.2}$-Pd
$Zn_4O(BDC\text{-}NH_2)_{1.2}(BDC)_{1.8}$-Pd
$Zn_4O(BDC\text{-}NH_2)_{0.6}(BDC)_{2.4}$-Pd
0 10 20 30 40 50
2θ (°)

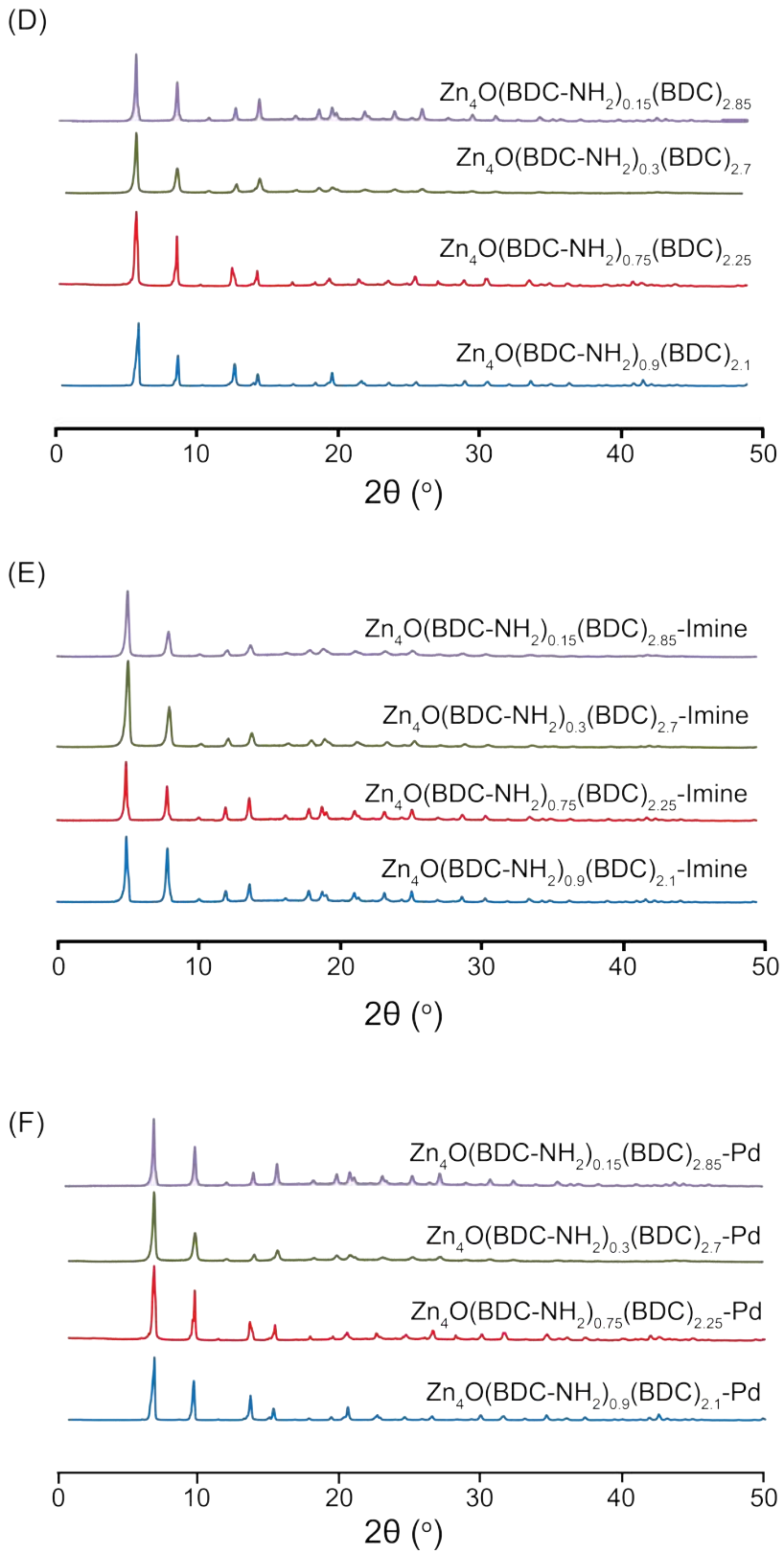

Figure S1. PXRD patterns of unfunctionalized (A, D), imine functionalized (B, E), and metalated frameworks (C, F).

Section S5: Gas adsorption at 77 K

Upon activation of $Zn_4O(BDC\text{-}NH_2)_n(BDC)_{(3-n)}$ (n = 3, 2.4, 1.8, 1.2, and 0.6), the N_2 isotherms of each material were measured at 77 K. Isotherms at 77 K indicated that metalation had decreased the porosity of $Zn_4O(BDC\text{-}NH_2)_3$-Pd, with the BET surface area of 210 m^2/g, analogous to other studies of metalation in $Zn_4O(BDC\text{-}NH_2)_3$.[S3] However, N_2 isotherms at 77 K confirmed other $Zn_4O(BDC\text{-}NH_2)_n(BDC)_{(3-n)}$ samples maintained high porosity upon metalation; the accuracy is 10 m^2/g for all samples. The maintenance of porosity displays the advantage of the application of the MTV-process in the metalation of MOFs with pores smaller than 1 nm. It is known that MOF samples after postsynthetic modification reactions sometimes show a significant hysteresis loop,[S3] and this is most likely due to intercrystalline voids in the sample related to lowered crystallinity of the sample after the postsynthetic modification reaction.[S4]

Low-pressure N_2 adsorption experiments (below 760 Torr) were performed on a Quantachrome NOVA 4200e automatic volumetric gas adsorption analyzer. Ultra-high purity grade N_2 (99.999% purity) and a liquid nitrogen bath (77 K) were used. For the estimation of surface areas, the BET method was applied using the adsorption branches of the N_2 isotherms assuming a N_2 cross-sectional area of 16.2 $Å^2$/molecule.

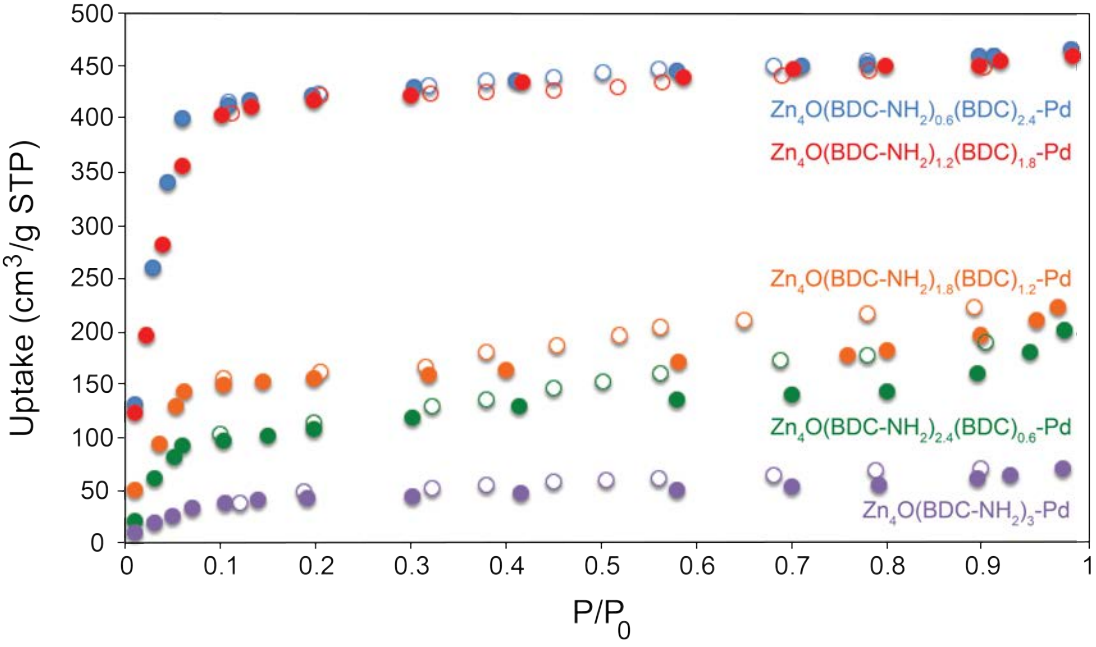

Figure S2. Representative N_2 isotherms of $Zn_4O(BDC\text{-}NH_2)_n(BDC)_{(3-n)}$-Pd samples.

Section S6: ^{15}N and ^{1}H solution NMR spectra and ICP-AES analysis

^{15}N cross polarization/magic angle spinning (CP/MAS) solid state nuclear magnetic resonance (NMR) provides no information about the yield of reactions; therefore, we employed digestion NMR and inductively coupled plasma mass spectroscopy (ICP-MS) to quantify the yield of postmodification and metalation techniques that have been used to quantify the yield of postmodification reactions in MOFs.[S5,S6] Samples of metalated MOFs were digested in DCl/DMSO-d_6, all visible peaks in the spectra were labeled with corresponding hydrogen atoms (letters A-F wherever possible) and the percentage amino-BDC and functionalization for each framework is shown in Table S1. To determine the loading of the frameworks with palladium inductively coupled plasma atomic emission spectroscopy (ICP-AES) was performed, and Zn_4O:Pd ratios of 1:0.4, 1:0.7, 1:1.0, 1:1.1, and 1:1.7 for $Zn_4O(BDC\text{-}NH_2)_{0.6}(BDC)_{2.4}$-Pd, $Zn_4O(BDC\text{-}NH_2)_{1.2}(BDC)_{1.8}$-Pd, $Zn_4O(BDC\text{-}NH_2)_{1.8}(BDC)_{1.2}$-Pd, $Zn_4O(BDC\text{-}NH_2)_{2.4}(BDC)_{0.6}$-Pd, and $Zn_4O(BDC\text{-}NH_2)_3$-Pd, respectively, could be determined. All ICP-AES measurements have a standard deviation of 10%. MOF samples were digested in DMSO-d_6/D_2O/DCl. Liquid-state nuclear magnetic resonance (NMR) spectra were performed on a Bruker AX 400 spectrometer.

Table S1. Percentage and degree of functionalization of amino-BDC in MTV-MOFs

Framework	Expected amino-BDC content (%)	Actual amino-BDC content (%)	Imine formation (% of amino-BDC functionalized)
$Zn_4O(BDC\text{-}NH_2)_{0.15}(BDC)_{2.85}$	5	5.08	90
$Zn_4O(BDC\text{-}NH_2)_{0.3}(BDC)_{2.7}$	10	9.97	90
$Zn_4O(BDC\text{-}NH_2)_{0.6}(BDC)_{2.4}$	20	20.17	80
$Zn_4O(BDC\text{-}NH_2)_{0.75}(BDC)_{2.25}$	25	24.95	80
$Zn_4O(BDC\text{-}NH_2)_{0.9}(BDC)_{2.1}$	30	30.20	85
$Zn_4O(BDC\text{-}NH_2)_{1.2}(BDC)_{1.8}$	40	40.10	80
$Zn_4O(BDC\text{-}NH_2)_{1.8}(BDC)_{1.2}$	60	59.06	90
$Zn_4O(BDC\text{-}NH_2)_{2.4}(BDC)_{0.6}$	80	79.69	90
$Zn_4O(BDC\text{-}NH_2)_3$	100	100	70

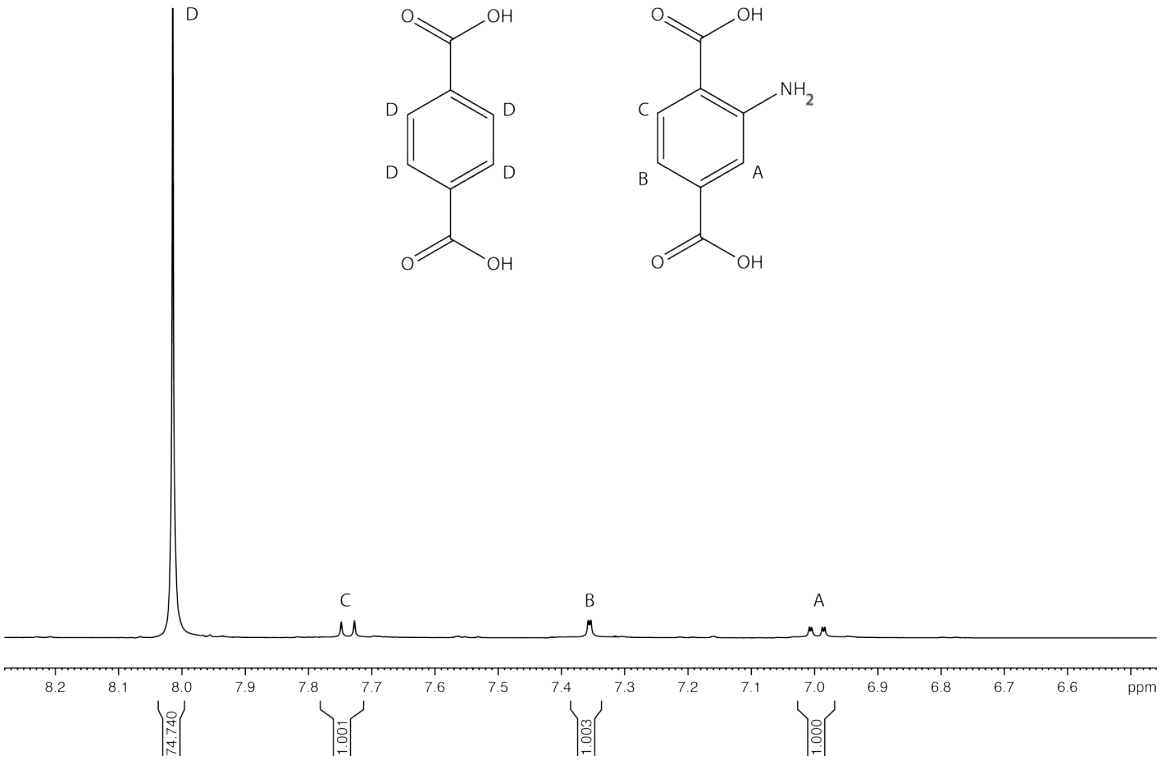

Figure S3. Digestion NMR spectrum of $Zn_4O(BDC\text{-}NH_2)_{0.15}(BDC)_{2.85}$.

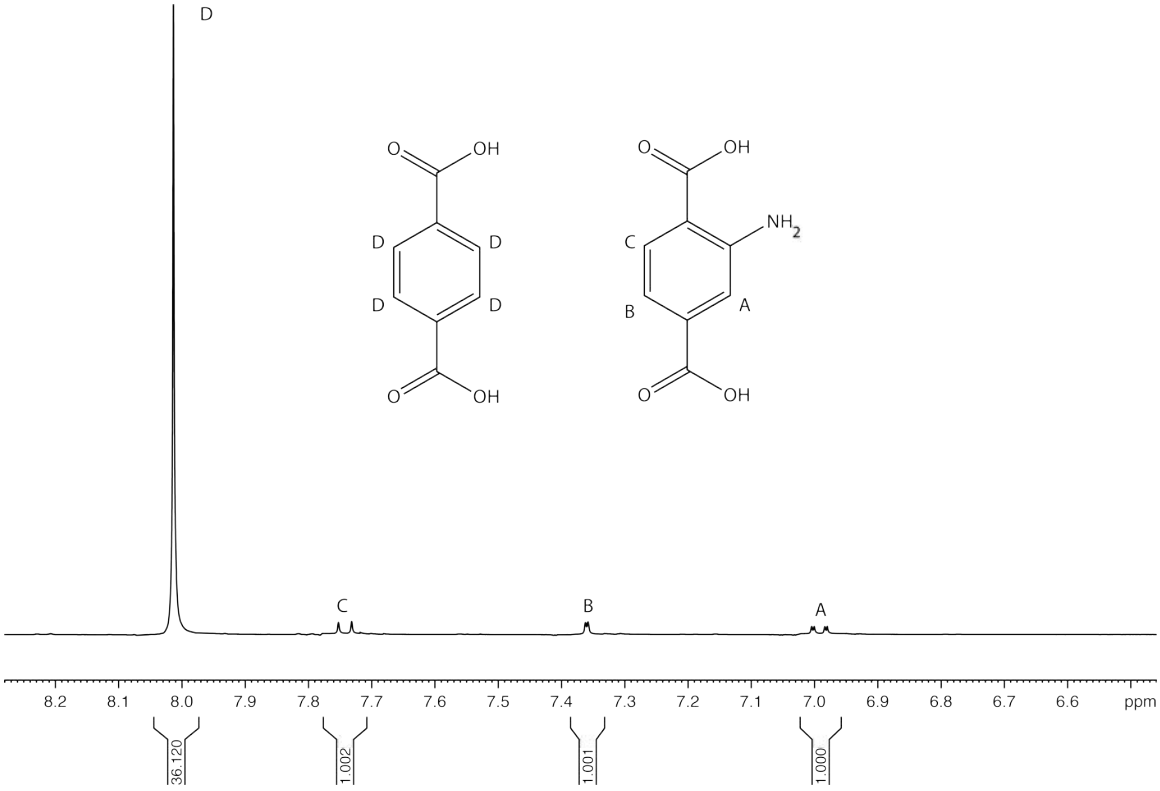

Figure S4. Digestion NMR spectrum of $Zn_4O(BDC\text{-}NH_2)_{0.3}(BDC)_{2.7}$

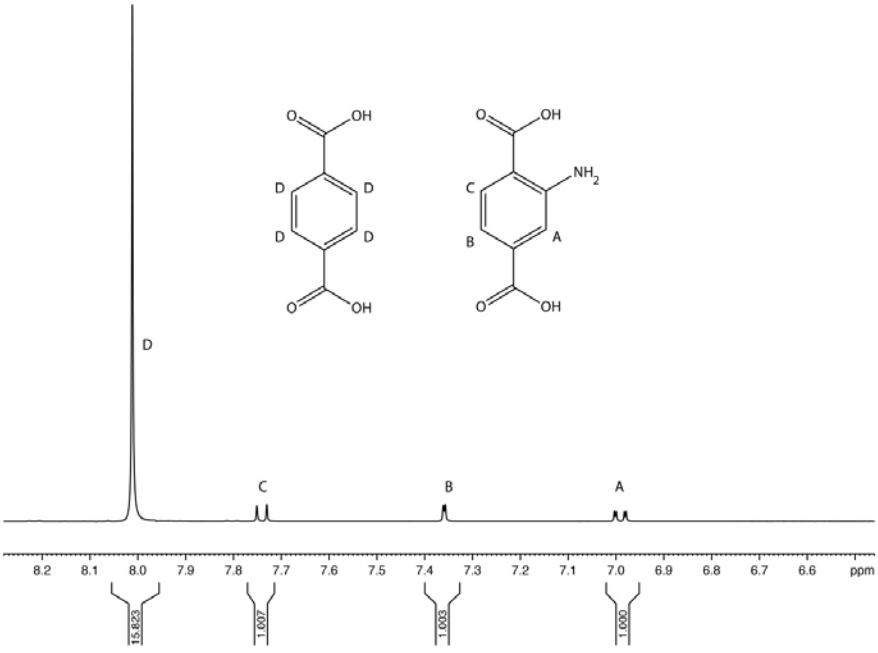

Figure S5. Digestion NMR spectrum of $Zn_4O(BDC\text{-}NH_2)_{0.6}(BDC)_{2.4}$.

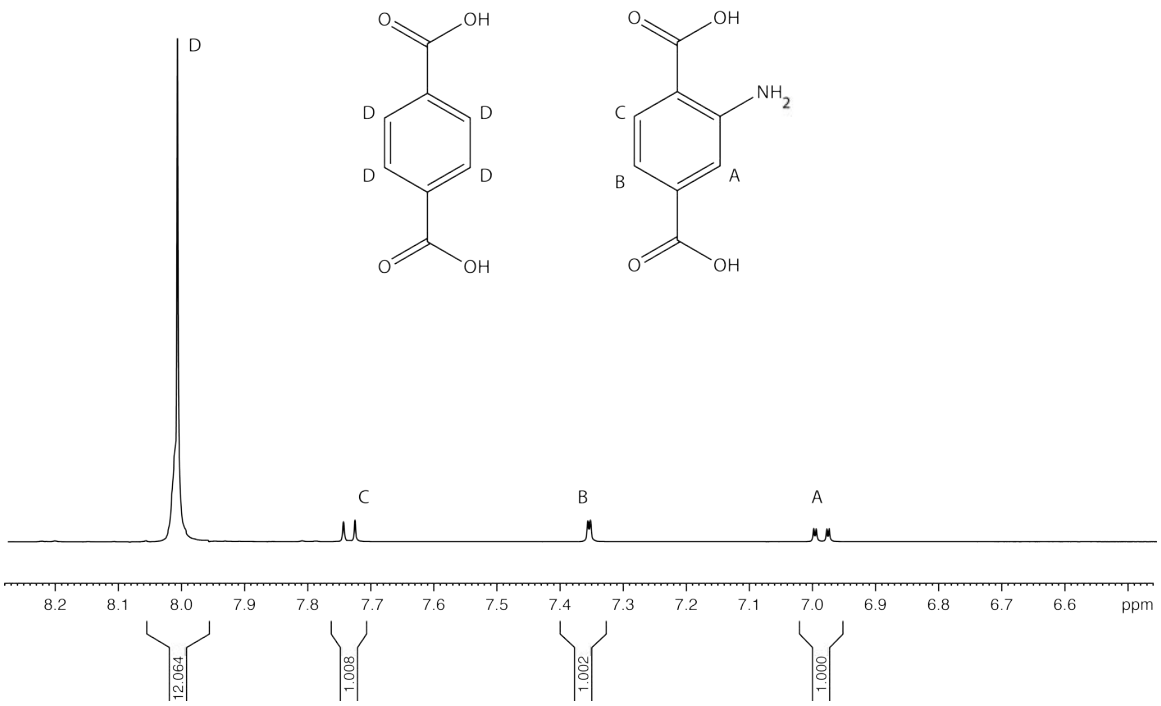

Figure S6. Digestion NMR spectrum of $Zn_4O(BDC\text{-}NH_2)_{0.75}(BDC)_{2.25}$.

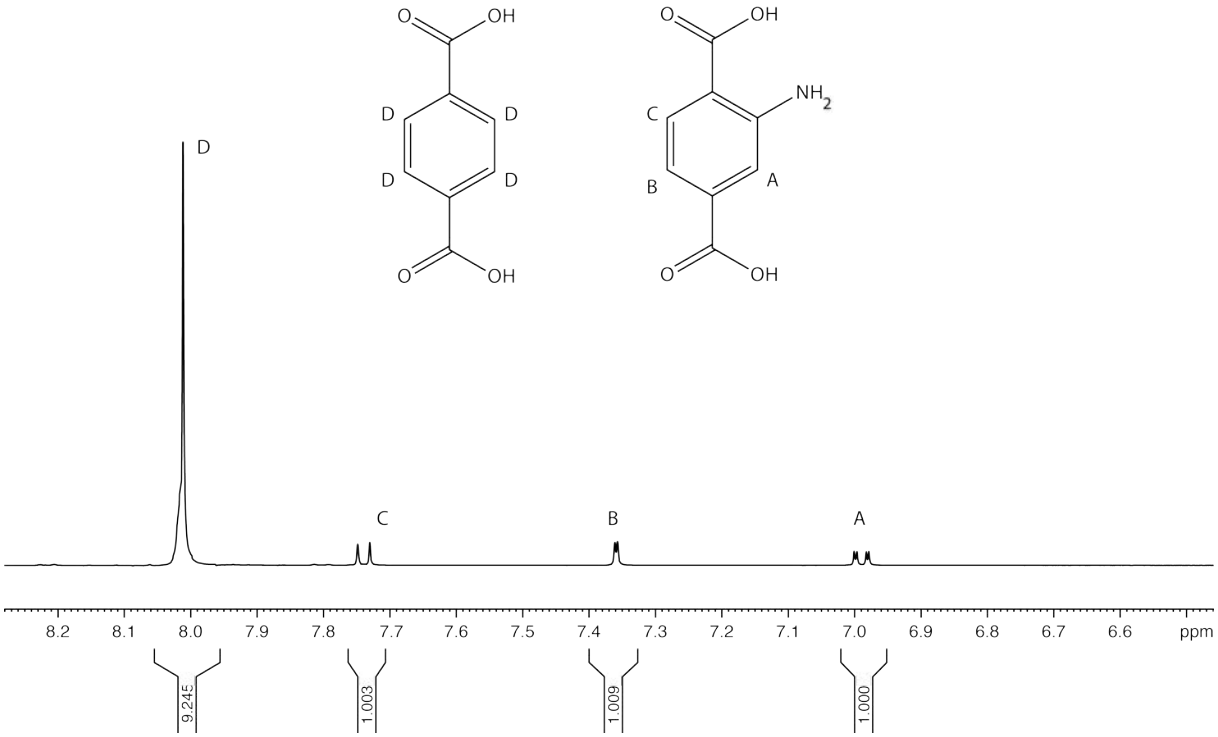

Figure S7. Digestion NMR spectrum of $Zn_4O(BDC\text{-}NH_2)_{0.9}(BDC)_{2.1}$

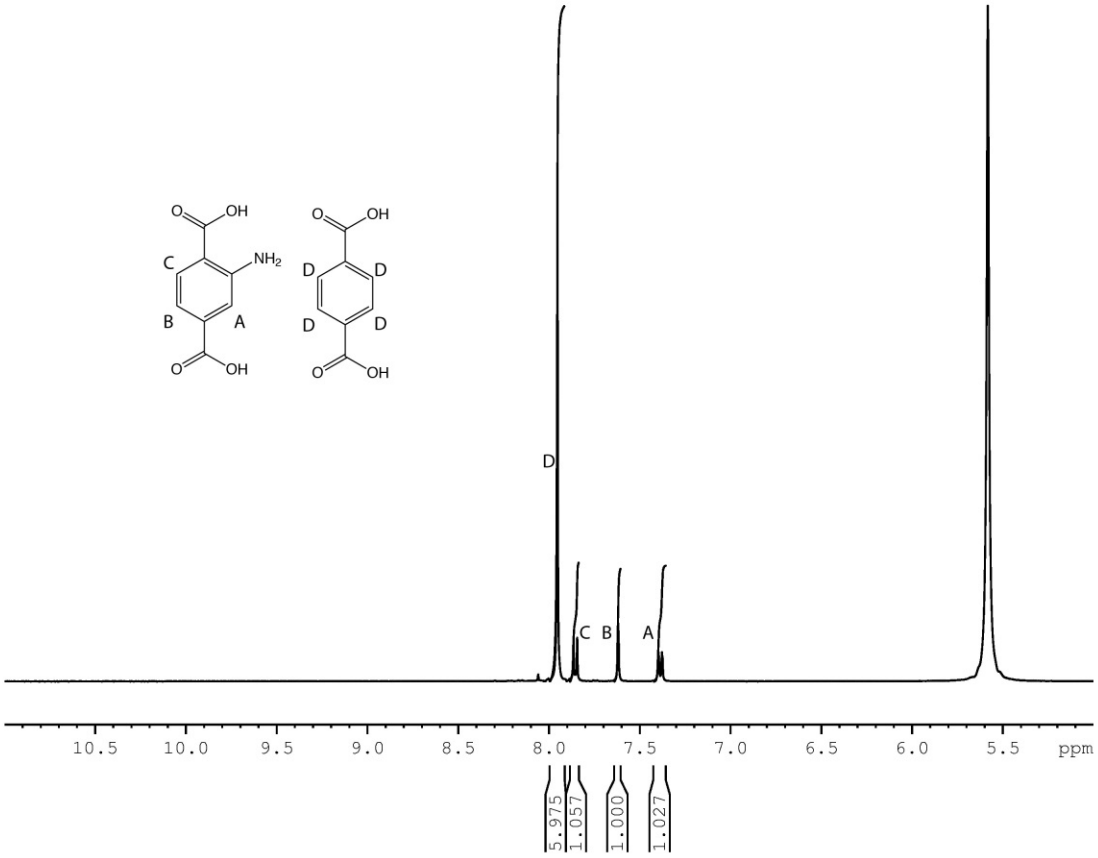

Figure S8. Digestion NMR spectrum of $Zn_4O(BDC\text{-}NH_2)_{1.2}(BDC)_{1.8}$.

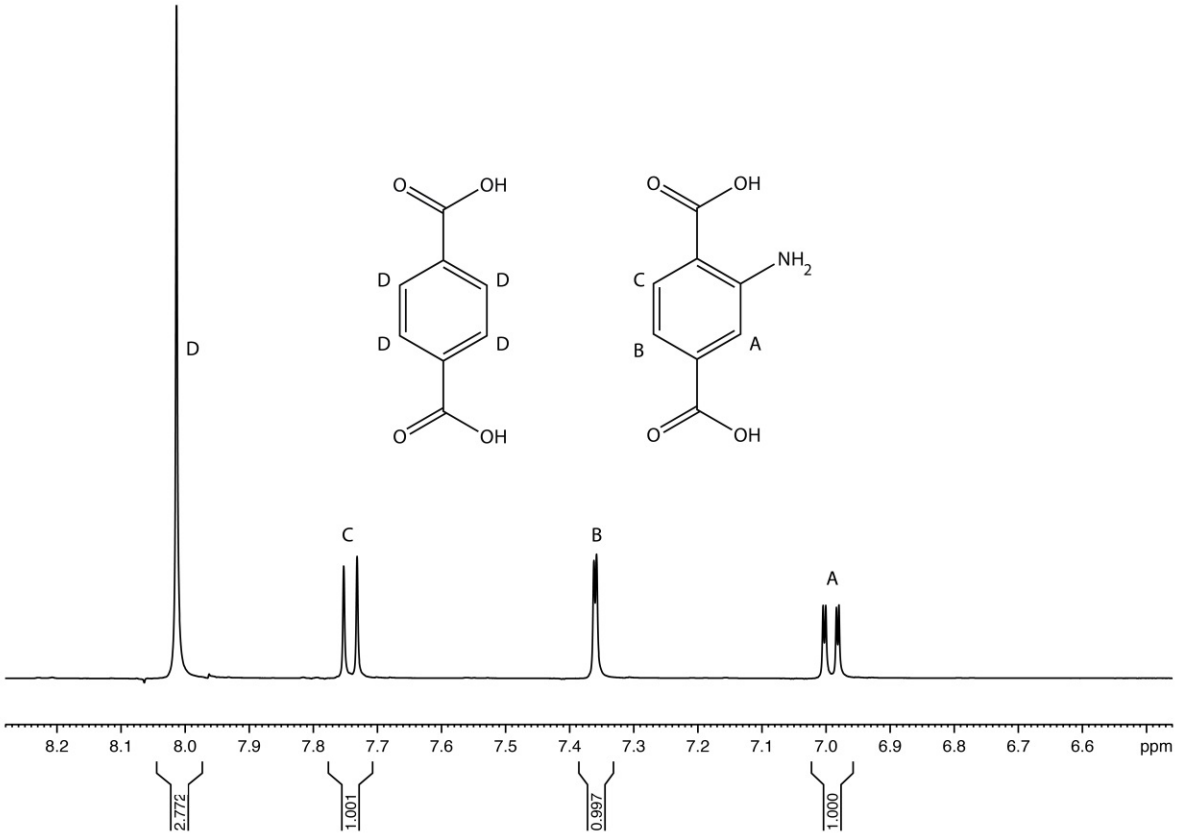

Figure S9. Digestion NMR spectrum of $Zn_4O(BDC\text{-}NH_2)_{1.8}(BDC)_{1.2}$.

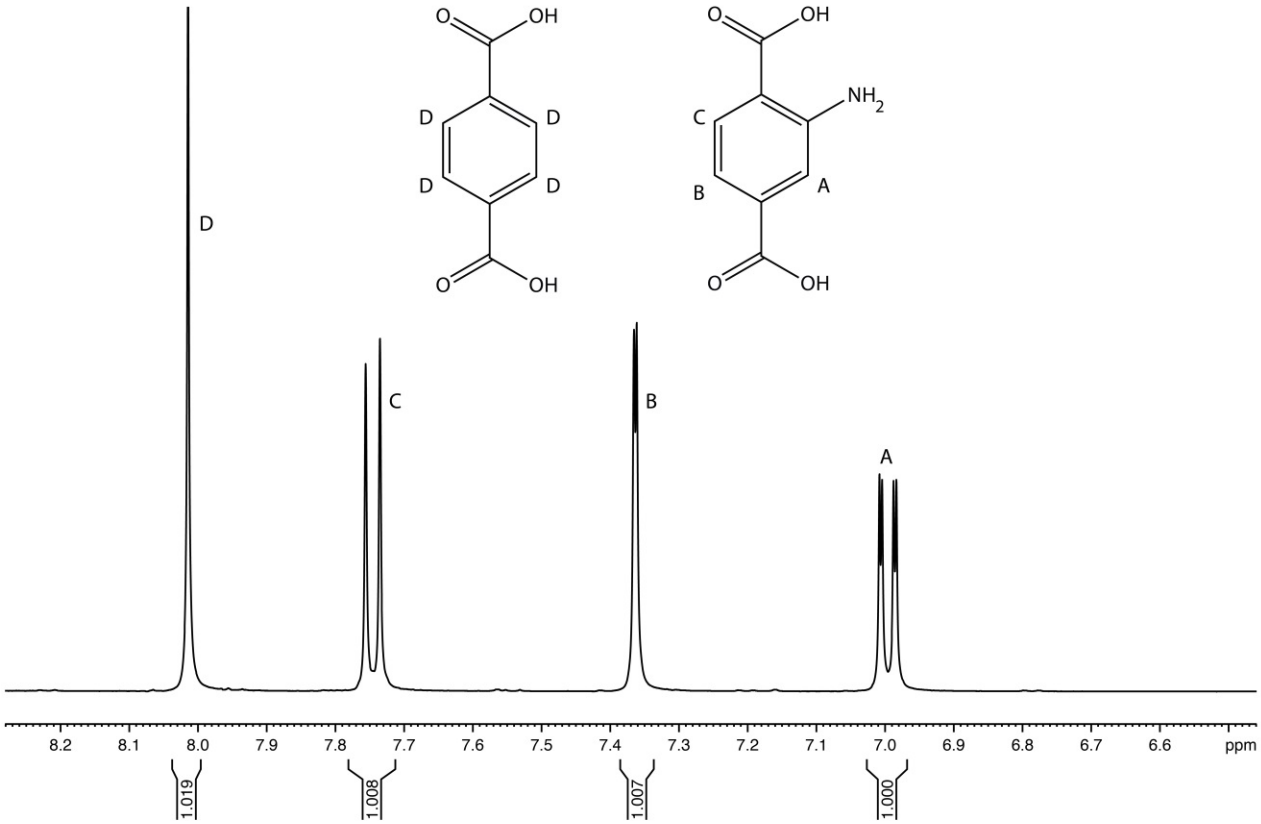

Figure S10. Digestion NMR spectrum of $Zn_4O(BDC\text{-}NH_2)_{2.4}(BDC)_{0.6}$.

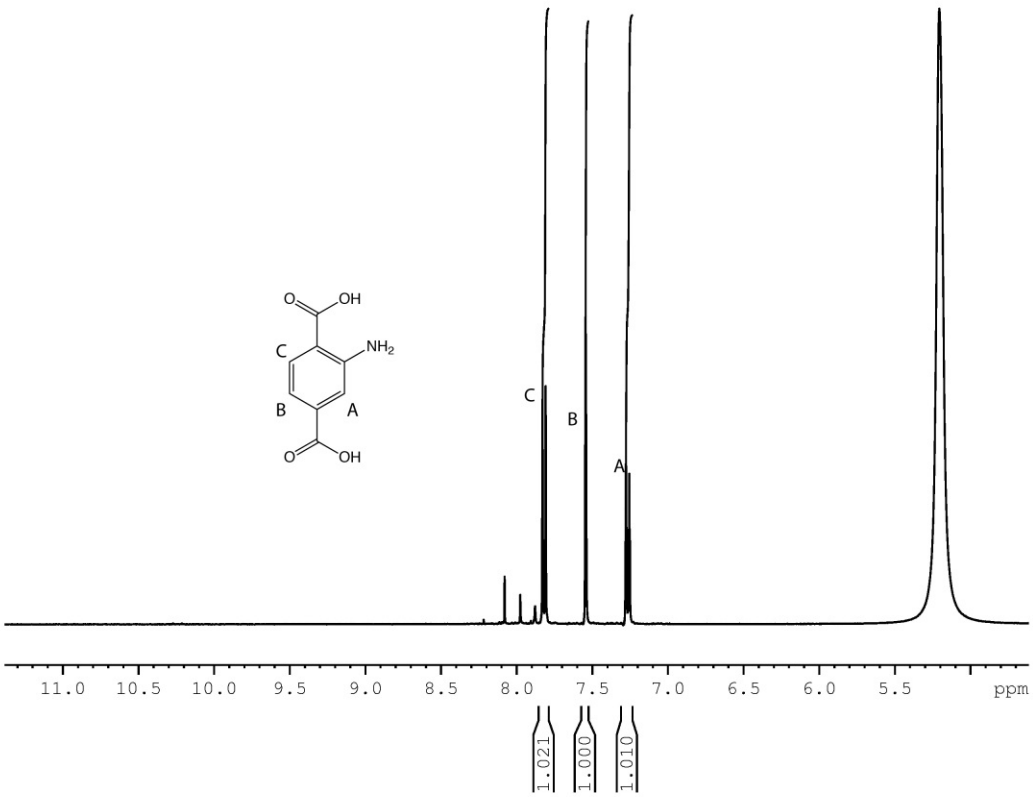

Figure S11. Digestion NMR spectrum of $Zn_4O(BDC\text{-}NH_2)_3$.

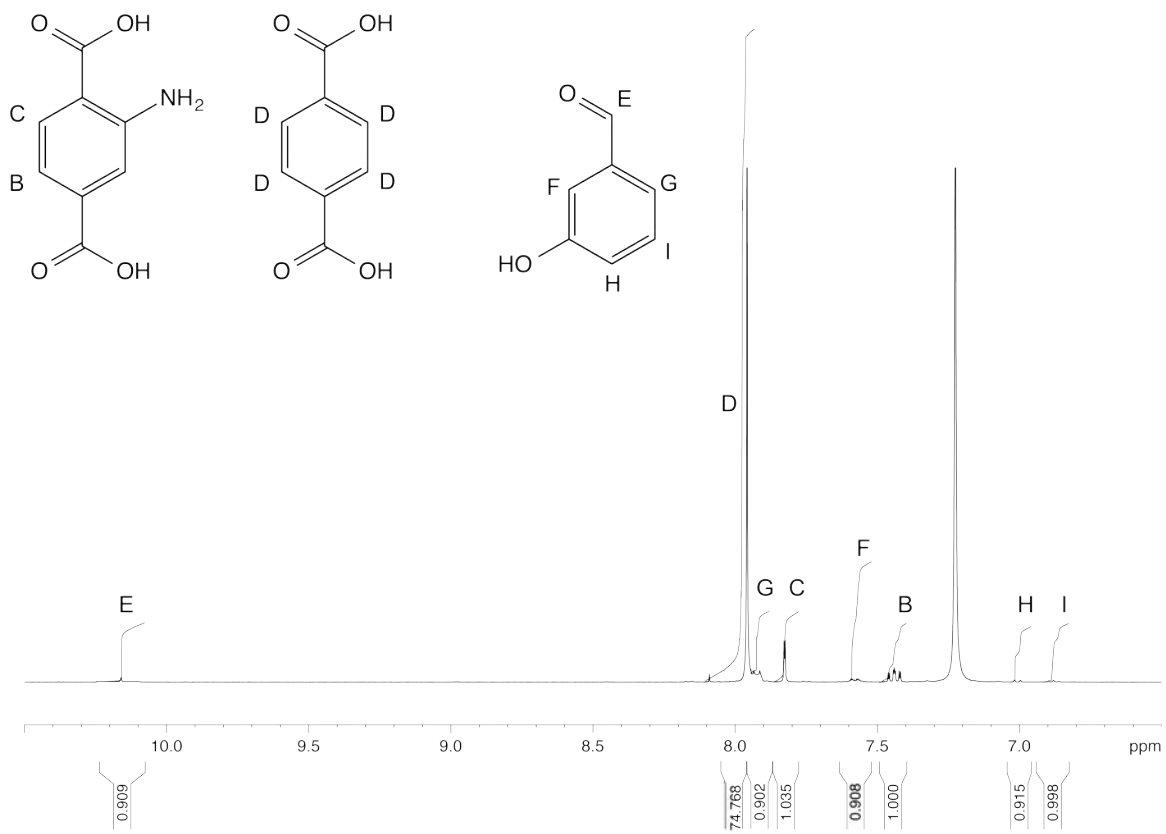

Figure S12. Digestion NMR spectrum of $Zn_4O(BDC\text{-}NH_2)_{0.15}(BDC)_{2.}$85-Pd.

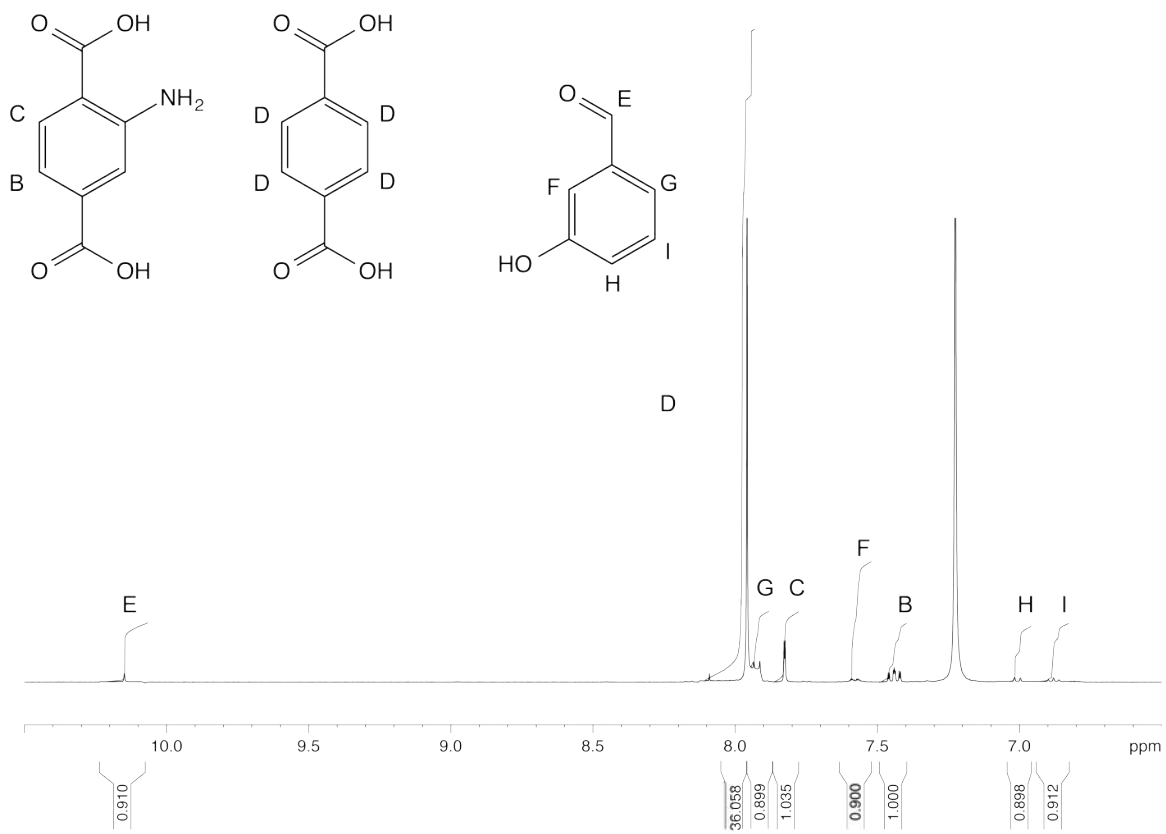

Figure S13. Digestion NMR spectrum of $Zn_4O(BDC\text{-}NH_2)_{0.3}(BDC)_{2.7}$-Pd.

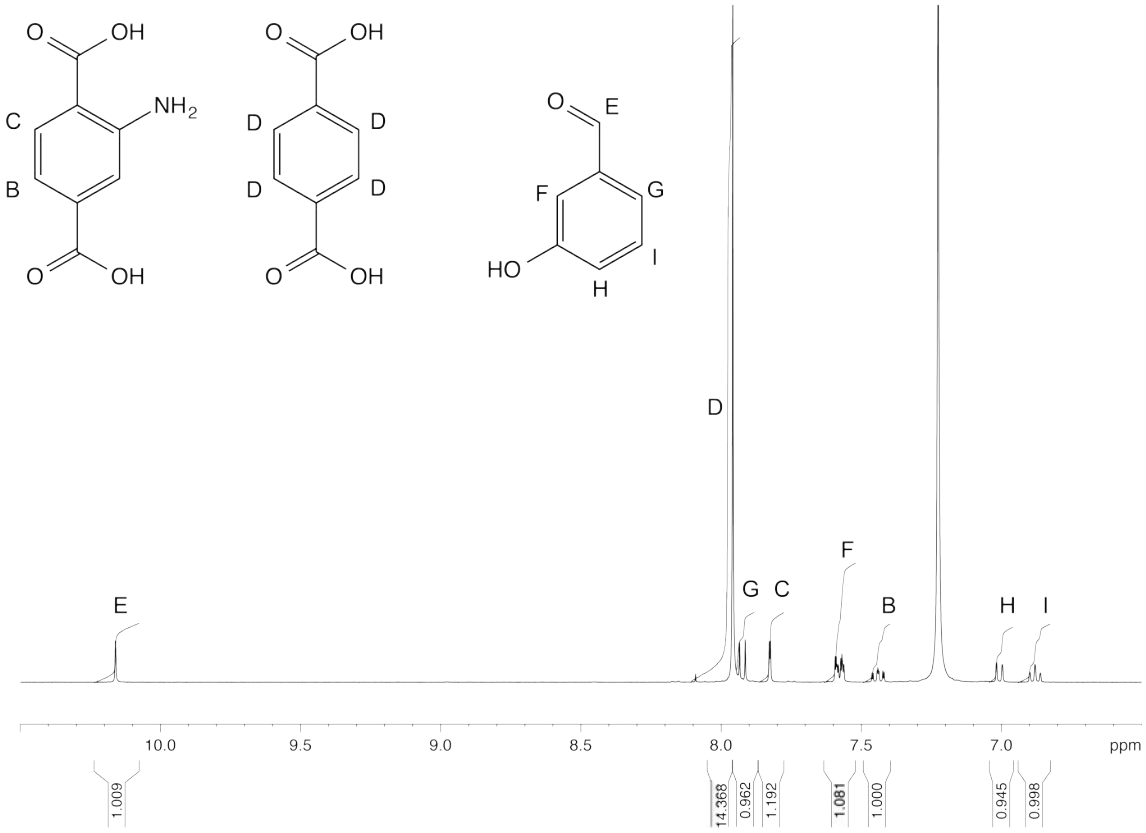

Figure S14. Digestion NMR spectrum of $Zn_4O(BDC\text{-}NH_2)_{0.6}(BDC)_{2.4}$-Pd.

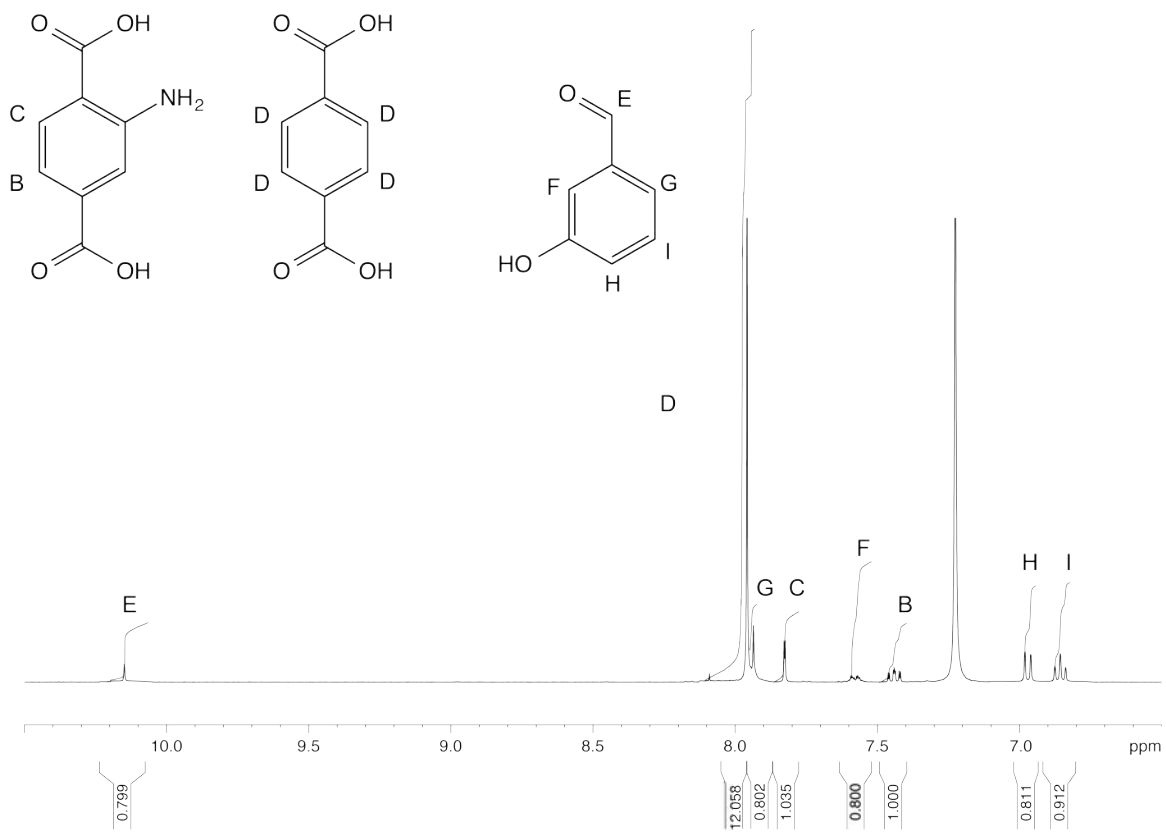

Figure S15. Digestion NMR spectrum of $Zn_4O(BDC\text{-}NH_2)_{0.75}(BDC)_{2.25}$-Pd.

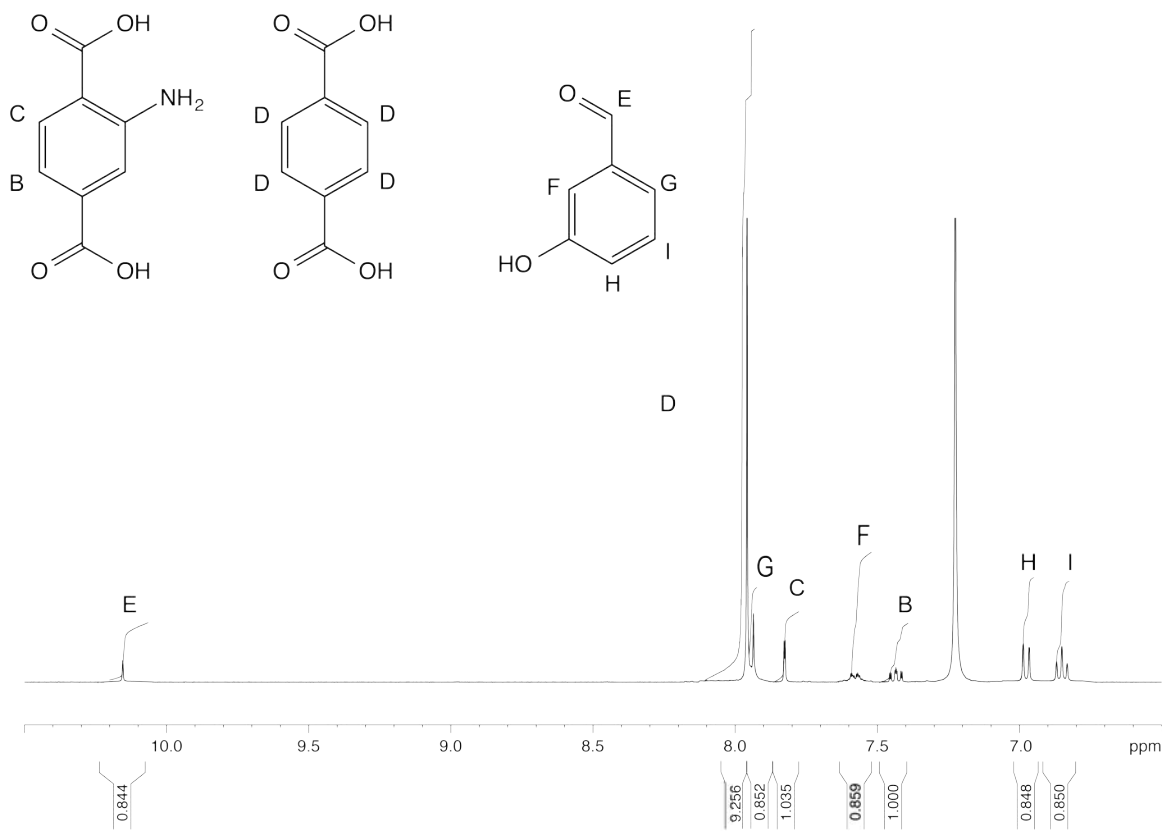

Figure S16. Digestion NMR spectrum of $Zn_4O(BDC\text{-}NH_2)_{0.9}(BDC)_{2.1}$-Pd.

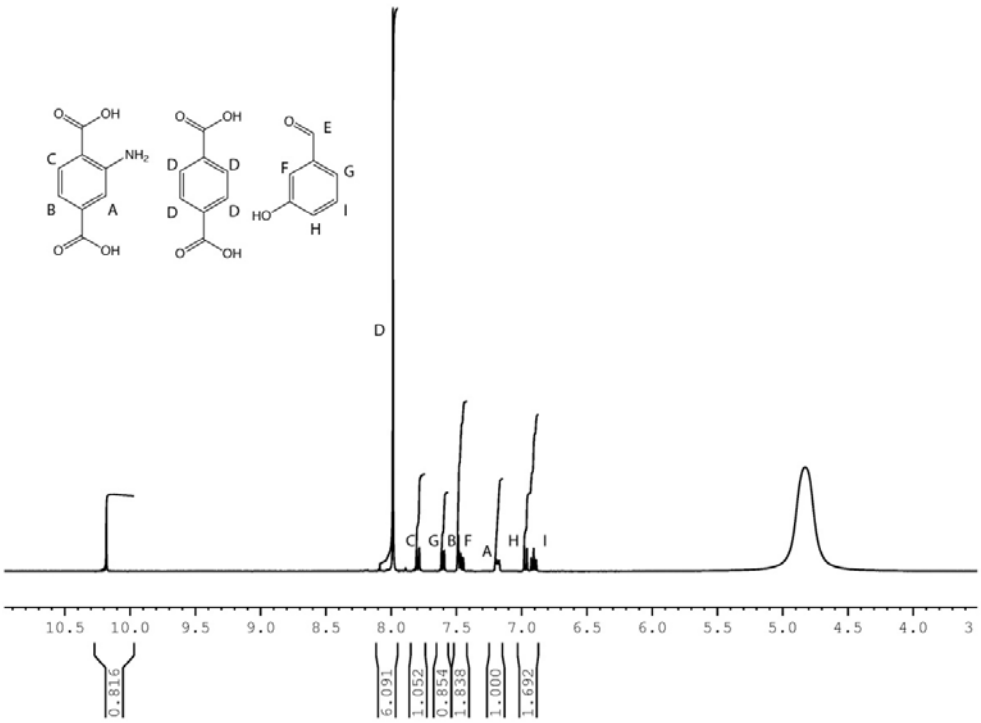

Figure S17. Digestion NMR spectrum of $Zn_4O(BDC\text{-}NH_2)_{1.2}(BDC)_{1.8}$-Pd.

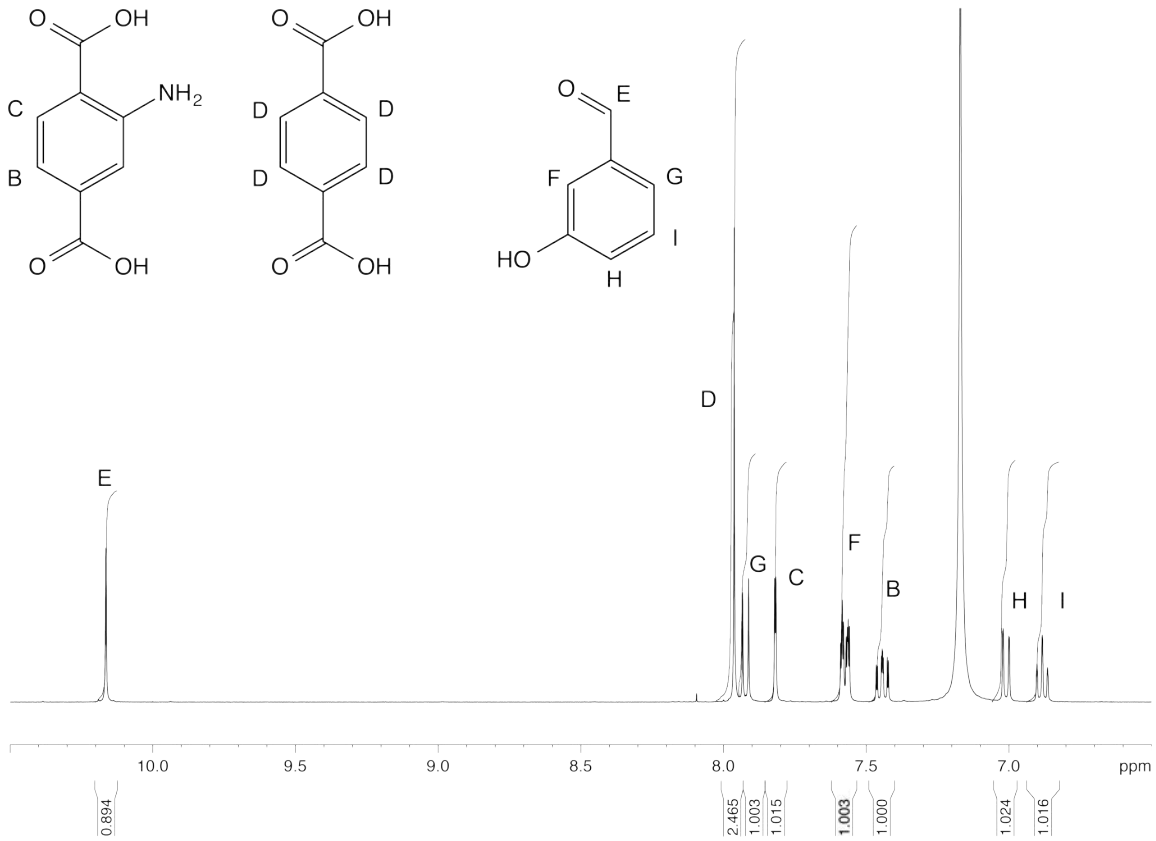

Figure S18. Digestion NMR spectrum of $Zn_4O(BDC\text{-}NH_2)_{1.8}(BDC)_{1.2}$-Pd.

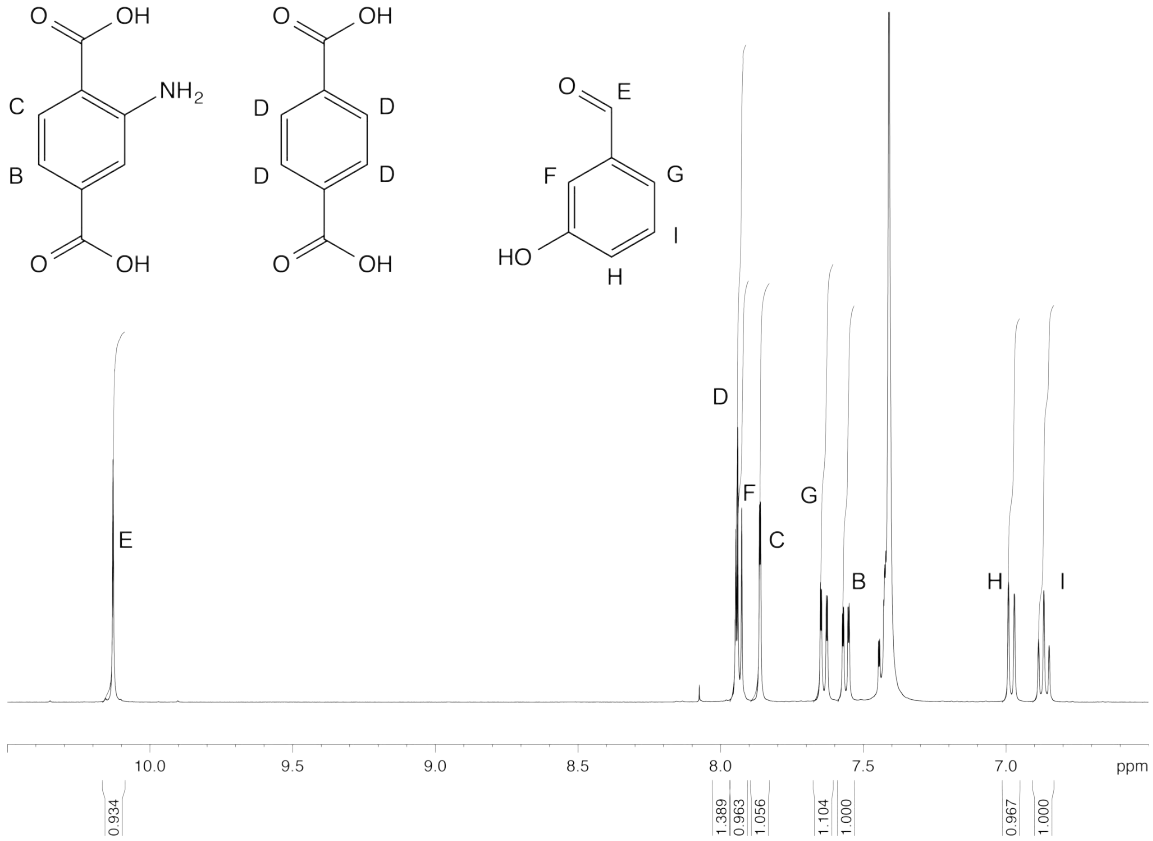

Figure S19. Digestion NMR spectrum of $Zn_4O(BDC\text{-}NH_2)_{2.4}(BDC)_{0.6}$-Pd.

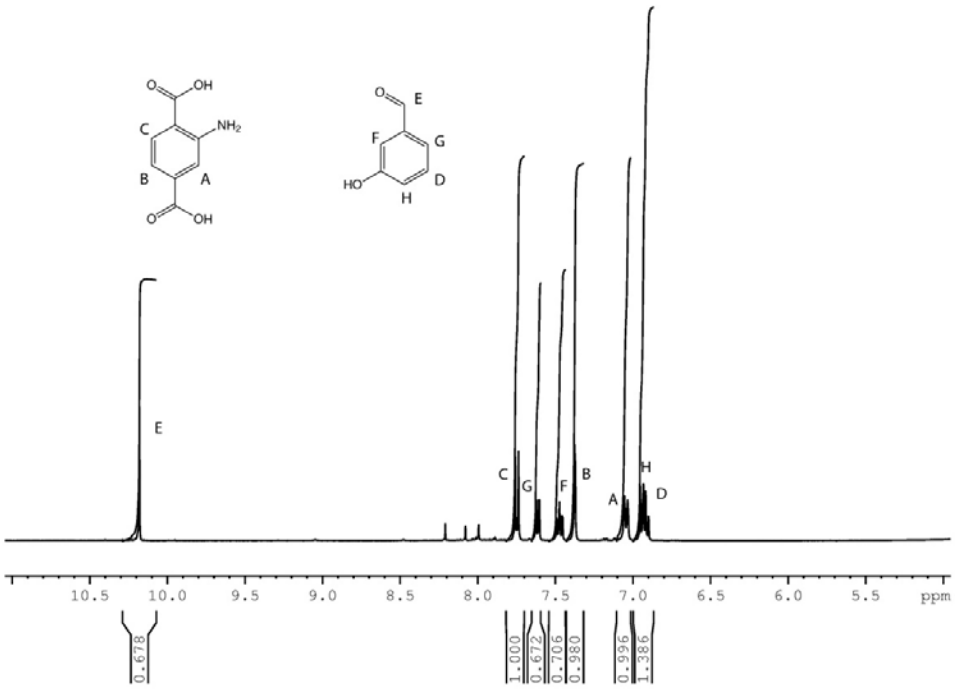

Figure S20. Digestion NMR spectrum of $Zn_4O(BDC\text{-}NH_2)_3$-Pd.

Section S7: Solid-state ^{15}N CP/MAS NMR spectroscopy.

The palladium coordination was determined using ^{15}N CP/MAS solid-state NMR spectroscopy, which characterizes the imine condensation and the metal binding site, with the use of ^{15}N labeled BDC-NH_2. $Zn_4O(BDC\text{-}NH_2)_{1.2}(BDC)_{1.8}$ was synthesized using labeled BDC-NH_2, ^{15}N CP/MAS solid-state NMR clearly showed an amine resonance at 65 ppm.[S7] Upon postmodification with salicyclic acid an imine resonance is observed at 255 ppm in $Zn_4O(BDC\text{-}NH_2)_{1.2}(BDC)_{1.8}$-Imine. In addition, the amine resonance is still observed at 68 ppm indicating the reaction does not proceed to completion. The final step of the postmodification in $Zn_4O(BDC\text{-}NH_2)_{1.2}(BDC)_{1.8}$, metalation, was further characterized by ^{15}N NMR, which contained a broad resonance at 10 ppm, the Pd-^{15}N bond of the imine complex. This resonance was confirmed by comparison to a model compound $Pd(C_{13}H_{10}NO)_2$, which also showed two resonances, at 5 and 13 ppm (Figure S13).

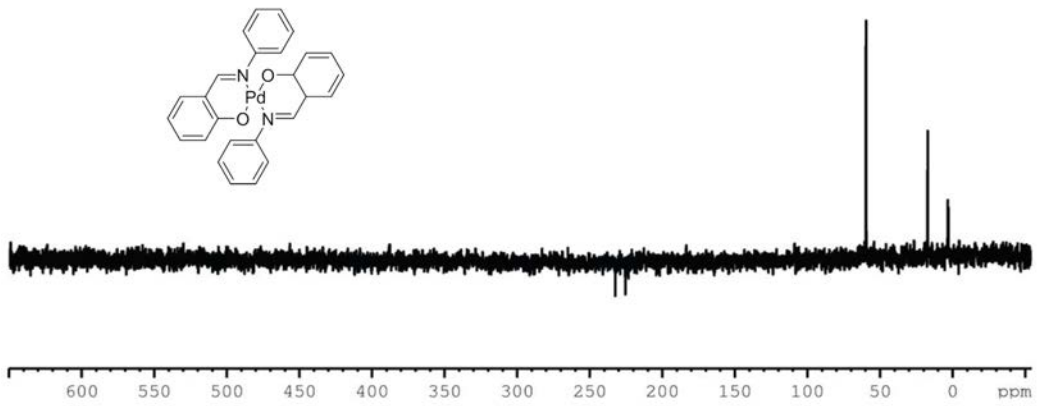

Figure S21. ^{15}N solution spectrum of a model compound $Pd(C_{13}H_{10}NO)_2$ used to confirm the metal binding in the solid state NMR experiments.

High resolution solid-state NMR spectra were recorded at ambient pressure on a Bruker DSX-300 spectrometer using a standard Bruker magic angle-spinning (MAS) probe with 4 mm (outside diameter) zirconia rotors. The magic angle was found by maximizing the number and amplitudes of the signals of the rotational echoes observed in the ^{79}Br MAS free induction signal from KBr.

^{15}N CP MAS for the isotopically labeled materials were measured at 30.42 MHz. The ^{1}H and ^{15}N ninety-degree pulse widths were both 4 μs. The CP contact time varied from 1.5 to 5 ms. The direct excitation NMR was measured at recycle delays of up to 45 seconds to allow for complete relaxation. The ^{15}N chemical shifts are given relative to liquid N_2 at zero ppm, calibrated using the nitrogen signal of glycine assigned to 36.2 ppm as secondary reference.

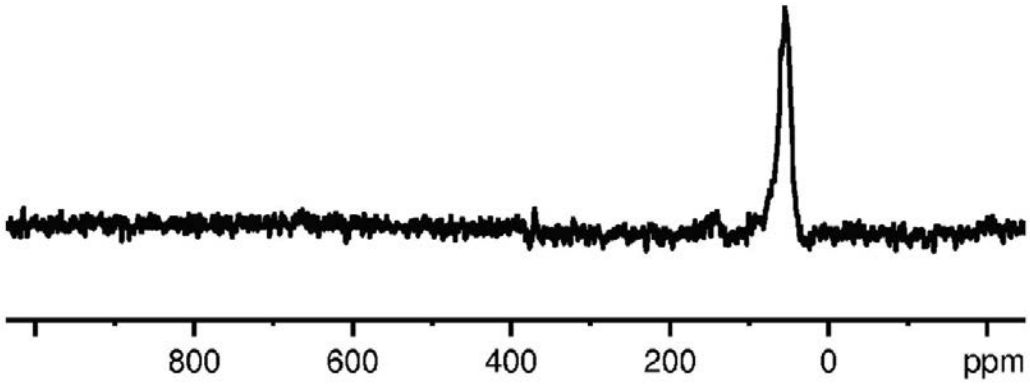

Figure S22. ^{15}N CP/MAS NMR spectrum of $Zn_4O(BDC\text{-}NH_2)_{1.2}(BDC)_{1.8}$.

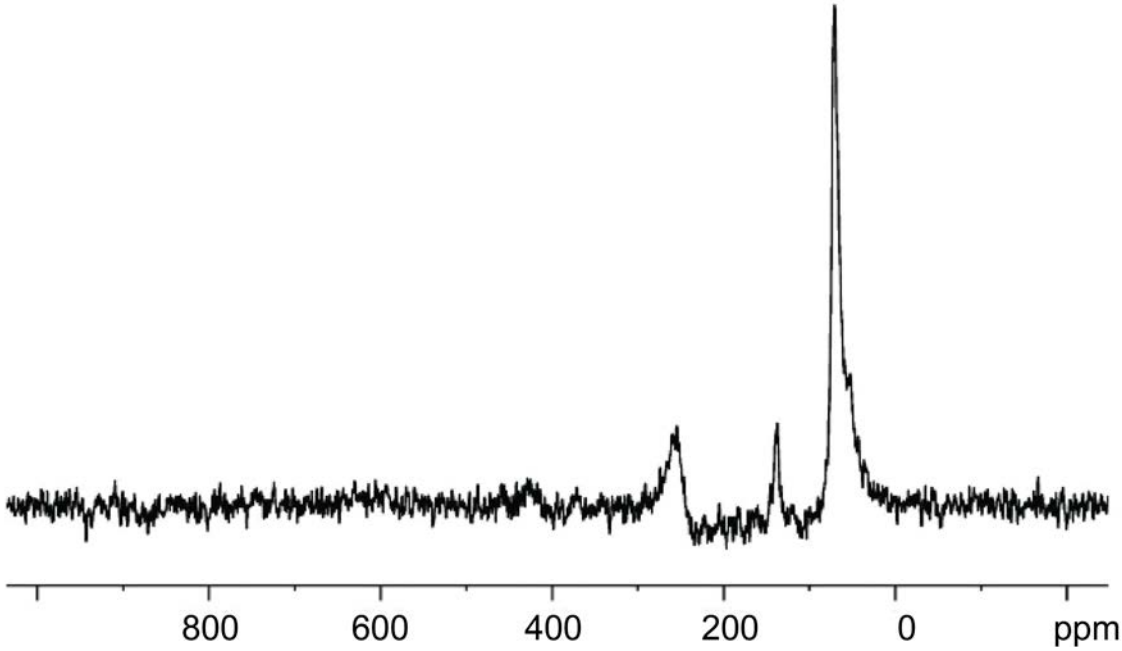

Figure S23. ^{15}N CP/MAS NMR spectrum of $Zn_4O(BDC\text{-}NH_2)_{1.2}(BDC)_{1.8}$-Imine. The peak between 100 and 200 is most likely the result of protonation of the amine. This downfield shift of approximately 100 ppm from the free amine has been observed by our group[S8] and other groups.[S9]

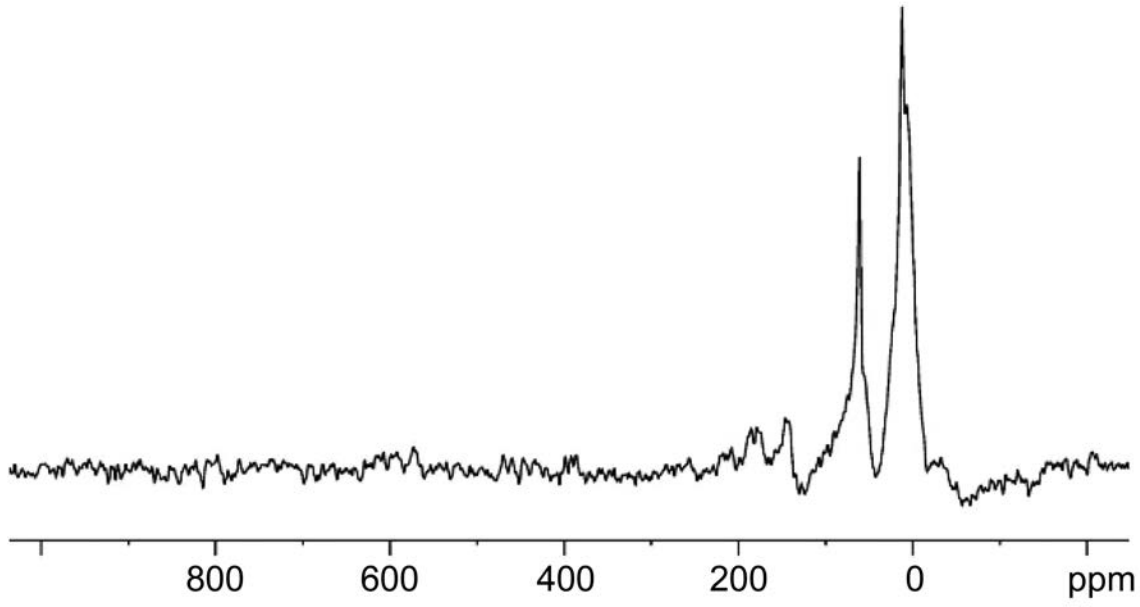

Figure S24. ^{15}N CP/MAS NMR spectrum of $Zn_4O(BDC\text{-}NH_2)_{1.2}(BDC)_{1.8}$-Pd.

Section S8: Optical microscopy

Optical microscopy of $Zn_4O(BDC\text{-}NH_2)_{1.2}(BDC)_{1.8}$, $Zn_4O(BDC\text{-}NH_2)_{1.2}(BDC)_{1.8}$-Imine, $Zn_4O(BDC\text{-}NH_2)_{1.2}(BDC)_{1.8}$-Pd was carried out using a Leica optical microscope. The as-synthesized samples were dispersed onto a glass plate for imaging.

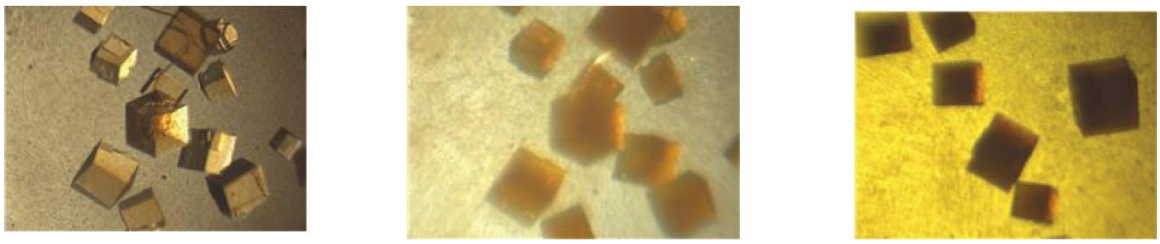

Figure S25. Optical microscopy of $Zn_4O(BDC\text{-}NH_2)_{1.2}(BDC)_{1.8}$, $Zn_4O(BDC\text{-}NH_2)_{1.2}(BDC)_{1.8}$-Imine, $Zn_4O(BDC\text{-}NH_2)_{1.2}(BDC)_{1.8}$-Pd, from left to right

Section S9: Catalytic Testing: Experimental Setup

In a 25 mL Schlenk flask, 1-bromo-3,5-methoxybenzene (0.434 g, 2 mmol), 4-vinylanisole (0.401 mL, 3 mmol), triethylamine (0.42 mL, 3 mmol), tetra-n-butylammonium bromide (0.32 mg, 1 mmol), MOF (20 mg), dodecane (1.0 mmol, inert

internal standard) were added to DMA (6 mL). After rapidly stirring for 5 minutes, the reaction was heated to 120 °C for 12 hours and was monitored via gas chromatography-mass spectroscopy (GC-MS).

Experiments with a palladium homogeneous catalyst used the following procedure:
In a 25 mL Schlenk flask, 1-bromo-3,5-methoxybenzene (0.434 g, 2 mmol), 4-vinylanisole (0.401 mL, 3 mmol), triethylamine (0.42 mL, 3 mmol), tetra-n-butylammonium bromide (0.32 mg, 1 mmol), $(MeCN)_2Pd(Cl)_2$ (10 mol%), dodecane (1.0 mmol, inert internal standard) were added to DMA (6 mL). After rapidly stirring for 5 minutes, the reaction was heated to 120 °C for 12 hours and was monitored via gas chromatography-mass spectroscopy (GC-MS).

Section S10: Determination of Catalytic Activity: GC-MS

Instrument description. GC-MS measurements were carried out using an Agilent Model 7683 Autosampler, 6890 Gas Chromatograph, and 5975 Inert Mass Selective Detector in the Electron Impact (EI) mode. EI energy was set to 70 eV. Data collection was controlled using MSD Enhanced Chemstation software (Agilent). Separation was carried out on an Agilent HP5-MS column with dimensions 30 m x 250 μm x 0.25 μm. Ultra High Purity Grade He (Airgas) was used as carrier gas with the flow set to 0.8 mL/min in constant flow mode.

Data collection parameters. 1 μL of sample dissolved in dichloromethane (Fisher) was injected using a split ratio of 20:1, with the inlet temperature set to 280 °C. The initial oven temperature was set to 45 °C for 1 minute followed by a 30 °C/min ramp to a final temperature of 300 °C which was maintained for 3 min. A 4.5 min solvent delay was used. The MSD was set to scan the 40 – 1050 m/z range.

Data analysis. Mass Spectrometric data was analyzed using the MSD Enhanced Chemstation software. Product spectra were identified by comparison of the measured fragmentation patterns to those found in the NIST 08 Mass Spectral Library.

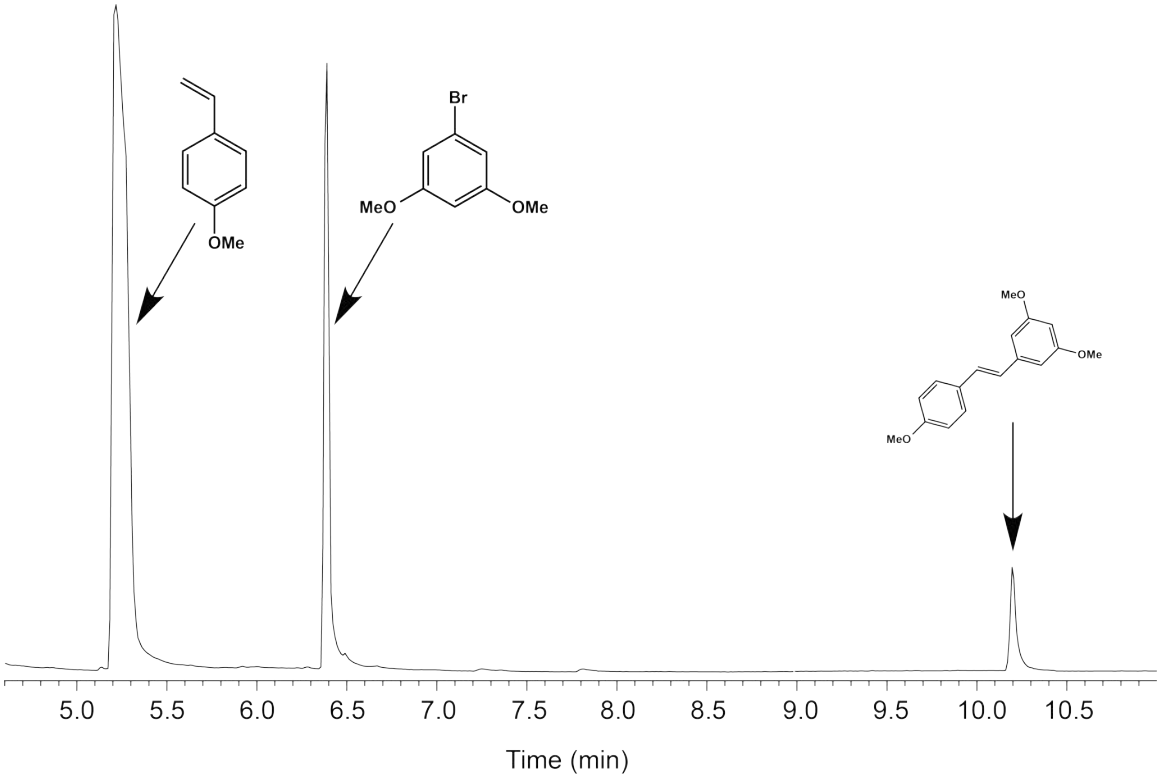

Figure S26. GC-MS of pure reactants and product for Heck coupling to establish retention times

To determine the retention times of the isomers of resveratrol trimethyl ether, a sample of trans-resveratrol trimethyl ether was placed under U. V. irradiation (294 nm for 60 mins). GC-MS experiments of the resveratrol trimethyl ether was performed both before and after irradiation and shown in Figures S19 and S20, respectively.

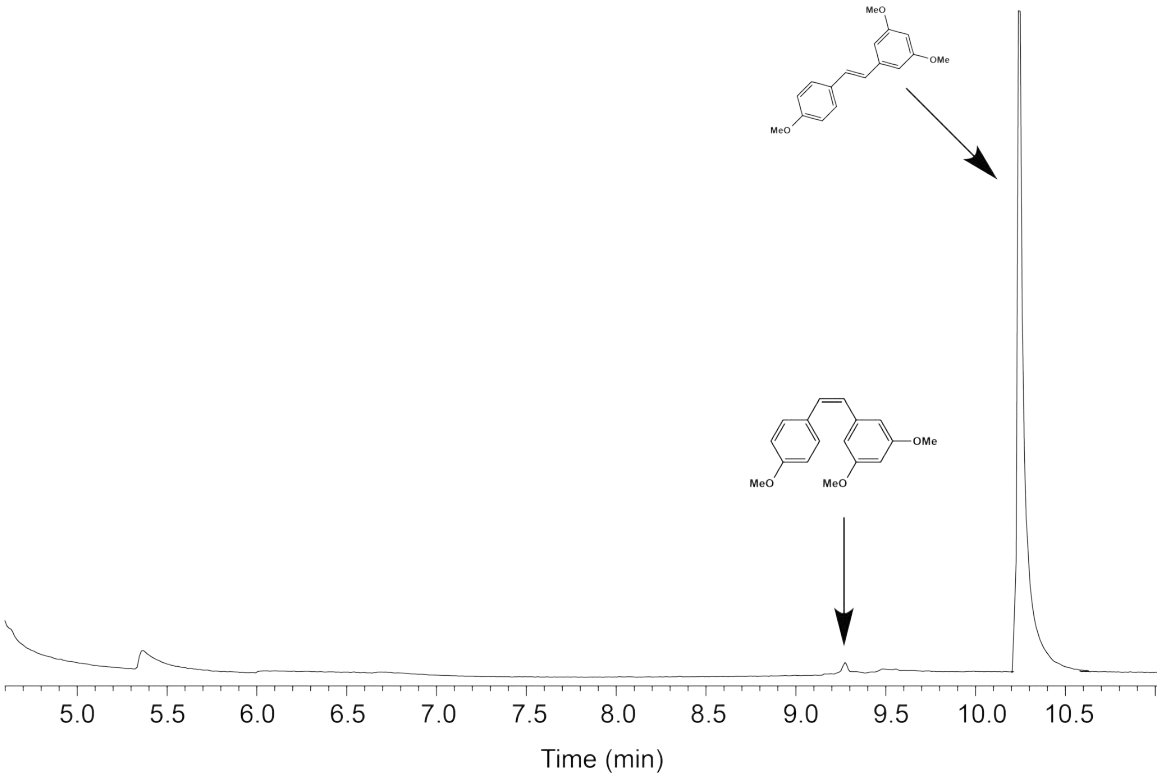

Figure S27. GC-MS of resveratrol trimethyl ether before U.V. irradiation (294 nm for 60 min)

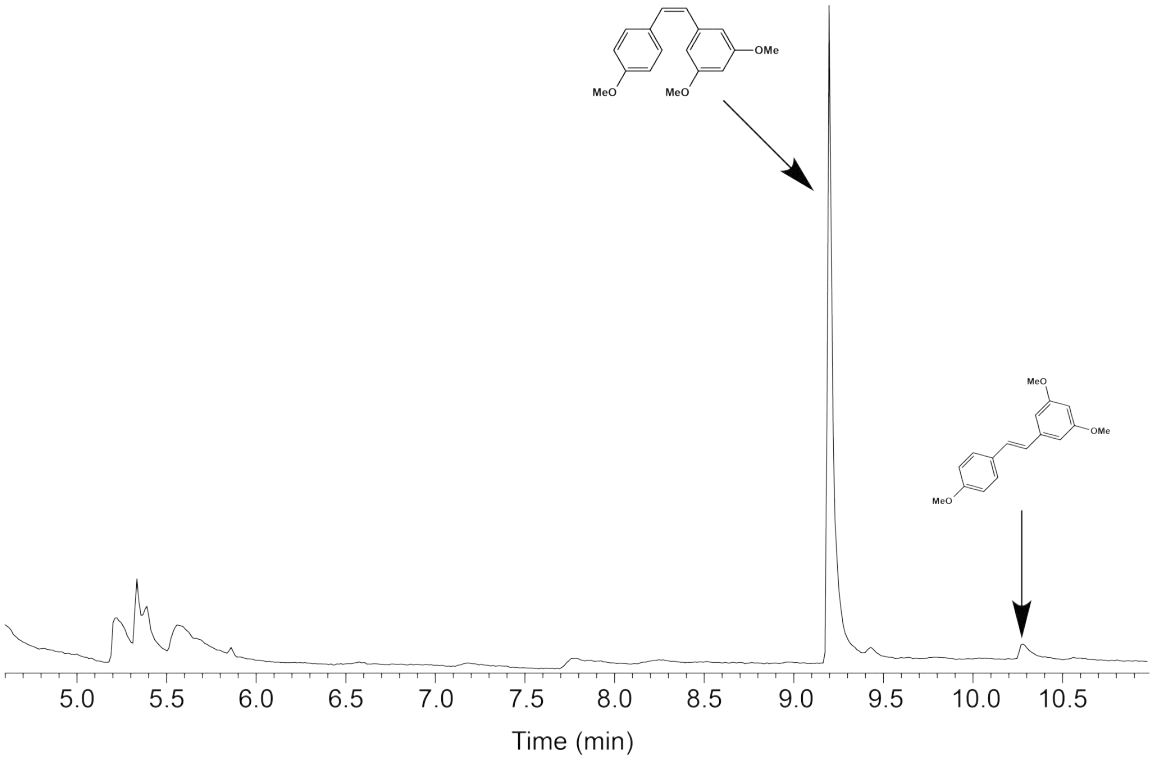

Figure S28. GC-MS of resveratrol trimethyl ether after U.V. irradiation

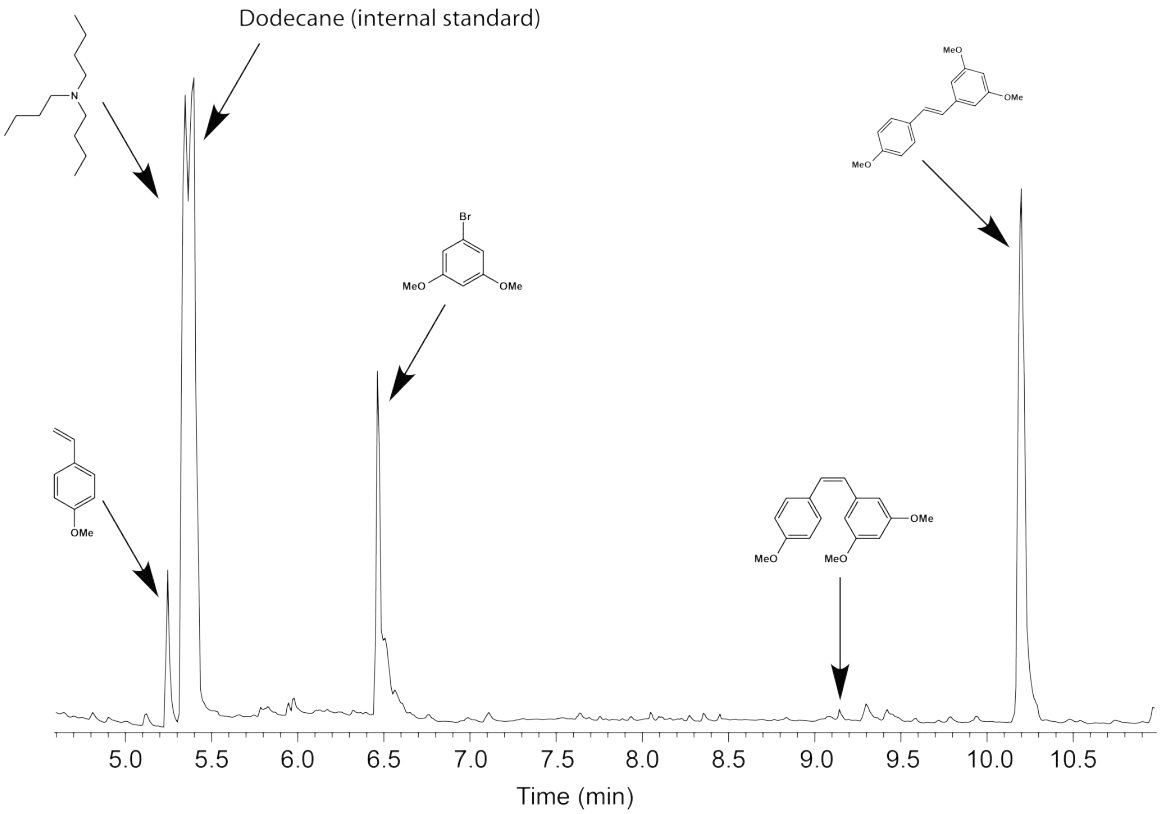

Figure S29. GC-MS of heck coupling reaction to synthesize resveratrol trimethyl ether

Section S11: Catalyst Results and Recycling Experiments

The yield and selectivity of all MOFs and a homogeneous palladium catalyst are shown in Table S2. We can see that some MOFs show higher yield and selectivity than the homogeneous catalyst.

Table S2. Yield and selectivity for MOF and homogeneous catalysts.

Catalyst used	Yield (%)	Trans to cis ratio in product
$Zn_4O(BDC\text{-}NH_2)_{0.6}(BDC)_{2.4}$	99.3 ± 0.02	105.9 :1
$Zn_4O(BDC\text{-}NH_2)_{1.2}(BDC)_{1.8}$	89.7 ± 1.7	81.9 : 1
$Zn_4O(BDC\text{-}NH_2)_{1.8}(BDC)_{1.2}$	75.5 ± 1.4	64.8 : 1
$Zn_4O(BDC\text{-}NH_2)_{2.4}(BDC)_{0.6}$	33.4 ± 3.8	53.9 : 1
$Zn_4O(BDC\text{-}NH_2)_3$	15.5 ± 1.6	46.6 : 1
$(MeCN)_2Pd(Cl)_2$	92.9 ± 0.9	58.5 : 1

Two MOFs [$Zn_4O(BDC\text{-}NH_2)_{0.6}(BDC)_{2.4}$-Pd and $Zn_4O(BDC\text{-}NH_2)_3$-Pd] were tested for recyclability to ensure that our frameworks maintain high yield after repeated catalytic cycles. As seen in Table S3, high catalytic activity and selectivity is maintained for 10 cycles.

Table S3. Average yield and trans to cis ratio of product for two MOFs after 10 catalytic cycles

Framework used	Average Yield for 10 cycles (%)	Average trans to cis ratio in product
$Zn_4O(BDC\text{-}NH_2)_{0.6}(BDC)_{2.4}$-Pd	99.3 ± 0.002	105.8 ± 6.3
$Zn_4O(BDC\text{-}NH_2)_3$-Pd	15.5 ± 1.6	46.5 ± 2.5

Section S12: Catalyst control and poisoning results

Control studies were performed to test that our metalated MOFs are the catalytically active species. Heck coupling reactions were run without any MOF present and with unmetalated MOFs to ensure that our frameworks without Pd are not catalytically active. As seen in Table S4, no catalytic conversion was observed if MOF is omitted or an unmetalated MOF is used. Reaction conditions, other than omitted species, are analogous to those of other catalytic runs, namely mixing MOF (20 mg), DMA (6 mL), 1-bromo-3,5-methoxybenzene (0.434 g, 2 mmol), 4-vinylanisole (0.401 mL, 3 mmol), triethylamine (0.42 mL, 3 mmol), tetra-n-butylammonium bromide (0.32 mg, 1 mmol), and dodecane (1.0 mmol, inert internal standard) . This mixture was stirred rapidly for 5 minutes before heating to 120 °C and monitoring the reaction via GC-MS.

Table S4. Reaction yields of Heck coupling after omission of MOF or using unmetalated MOF

Framework used	Yield (%) Unmetalated MOF	Yield (%) MOF omitted
$Zn_4O(BDC\text{-}NH_2)_{0.6}(BDC)_{2.4}$	0.0	0.0
$Zn_4O(BDC\text{-}NH_2)_{1.2}(BDC)_{1.8}$	0.0	0.0
$Zn_4O(BDC\text{-}NH_2)_{1.8}(BDC)_{1.2}$	0.0	0.0
$Zn_4O(BDC\text{-}NH_2)_{2.4}(BDC)_{0.6}$	0.0	0.0
$Zn_4O(BDC\text{-}NH_2)_3$	0.0	0.0

Catalyst poisoning experiments were performed to test that our metalated MOFs have a single site Pd catalyst and that Pd nanoparticles or aggregates have not formed during catalyst synthesis. Heck coupling reactions were run using $Zn_4O(BDC\text{-}NH_2)_{0.6}(BDC)_{2.4}$-Pd with the addition of either Hg(0) or PPh_3. As seen in Figure S30, no change in catalytic conversion was observed if Hg(0) is added to our reaction mixture. Figure S31 shows immediate drop-off of catalytic activity followed by cessation of all catalytic activity.

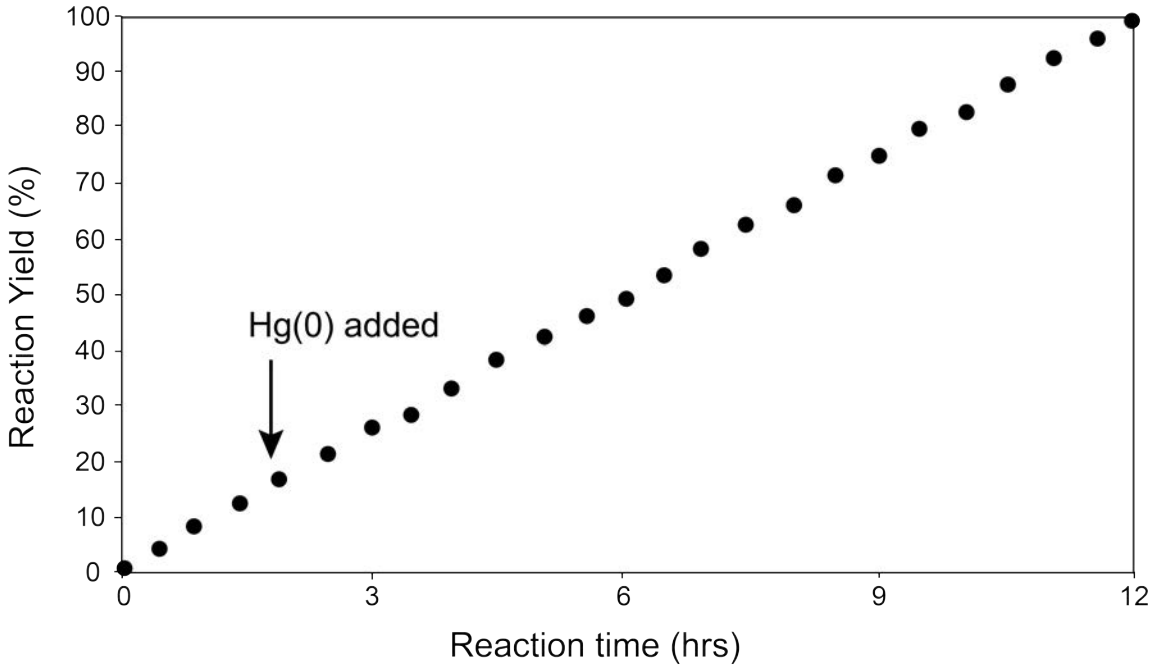

Figure S30. Reaction progress shows no change after Hg(0) is added to reaction mixture

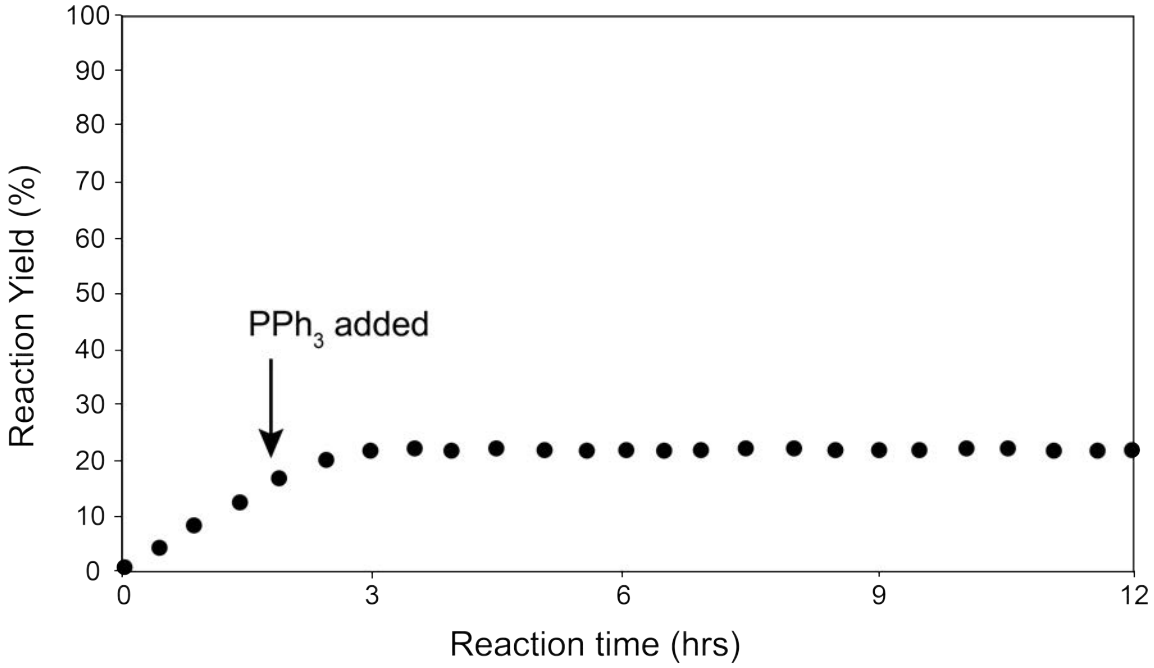

Figure S31. Reaction progress shows loss of catalytic activity after after PPh_3 is added to reaction mixture

Reaction conditions are analogous to those of other catalytic runs, namely mixing MOF (20 mg), DMA (6 mL), 1-bromo-3,5-methoxybenzene (0.434 g, 2 mmol), 4-vinylanisole

(0.401 mL, 3 mmol), triethylamine (0.42 mL, 3 mmol), tetra-n-butylammonium bromide (0.32 mg, 1 mmol), and dodecane (1.0 mmol, inert internal standard). For Hg(0) poisoning experiments, 0.25mL Hg(0) was added to the reaction mixture and for PPh_3 poisoning experiments, 80mg of PPh_3 was added to the reaction mixture. These mixtures was stirred rapidly for 5 minutes before heating to 120 °C and monitoring the reaction via GC-MS.

Section S13: ICP-AES of reaction product

Samples of the reaction product were submitted to USC to determine palladium leaching after the Heck coupling reaction had occurred. ICP-AES (standard deviation = 2.8%) indicated leaching was within the experimental error of the experiment and we conclude that no leeching occurred during the Heck coupling reaction.

Section S14: X-ray photoelectron spectroscopy (XPS)

X-ray photoelectron spectroscopy (XPS) was employed to investigate the oxidation state of the Pd in $Zn_4O(BDC\text{-}NH_2)_{1.2}(BDC)_{1.8}$-Pd and $Zn_4O(BDC\text{-}NH_2)_3$-Pd. In both samples only photoelectrons corresponding to Pd^{2+} are observed prior to catalysis, as expected for a square planar complex (Figure S21). However, after catalytic tests, XPS reveals both MOF samples contain Pd^{2+} and Pd^0, indicating that during the reaction, Pd^{2+} is reduced (Figure S21). This reduction is also observed in a color change from purple to black in each MOF sample. X-ray photoelectron spectroscopy (XPS) was performed using a Kratos AXIS Ultra DLD (acquired under NSF CRIF:MU award number 0840531) with the charge neutralizer on. The finely powdered samples were supported using non-conductive double-sided tape. Spectra were analyzed using CasaXPS, fitting the peak areas to a Gaussian/Lorentzian (GL(30)) product form lineshape (m = p/100, in which p = 30) (Figure S21(inset)). Pd *3d* spectra were fitted and plotted using the GL(30) lineshape.

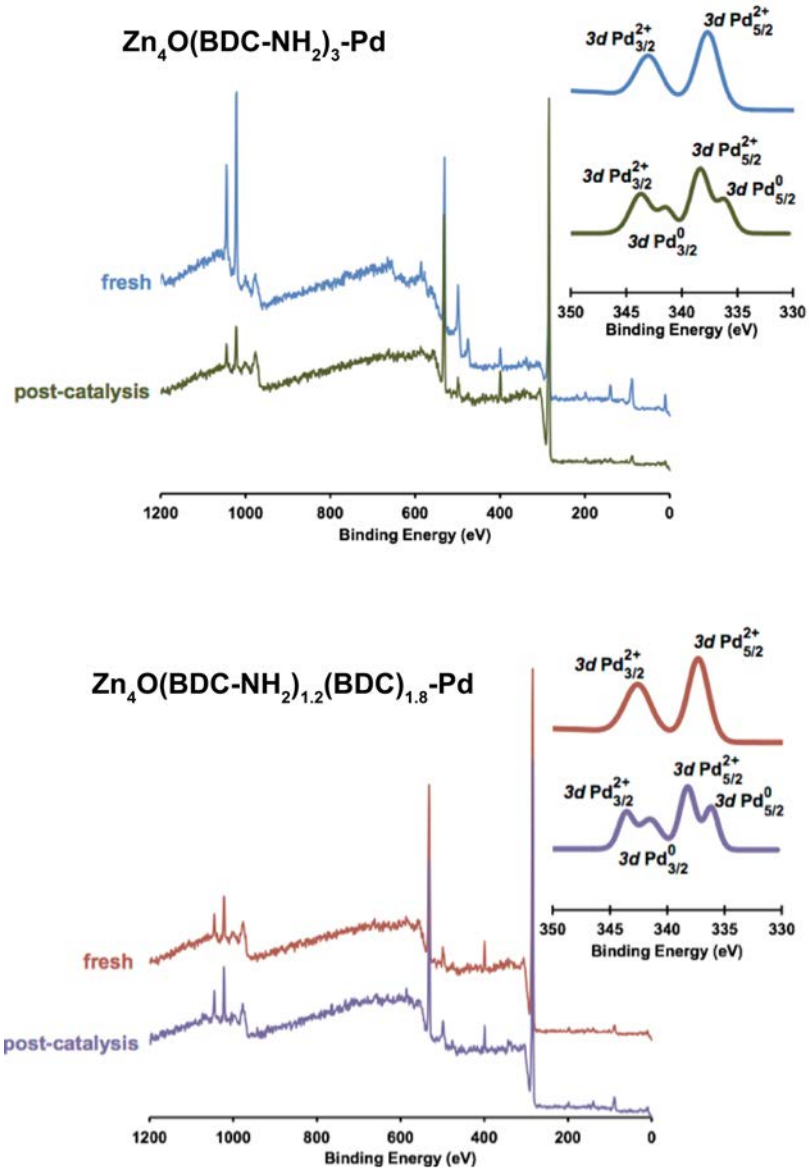

Figure S32. XPS Spectra of $Zn_4O(BDC\text{-}NH_2)_3$-Pd and $Zn_4O(BDC\text{-}NH_2)_{1.2}(BDC)_{1.8}$-Pd.

Section S15: References

(S1) M. Eddaoudi, J. Kim, N. Rosi, D. Vodak, J. Wachter, M. O'Keeffe, O. M. Yaghi, *Science* 2002, **295**, 469.

(S2) M. J. Ingleson, J. P. Barrio, J. -B. Guilbaud, Y. Z. Khimyak, M. J. Rosseinsky, *Chem. Commun.* 2008, **23**, 2680.

(S3) C. J. Doonan, W. Morris, H. Furukawa, O. M. Yaghi, *J. Am. Chem. Soc.* 2009, **131**, 9492.

(S4) A. Vishnyakov, P. T. Ravikovitch, A. V. Neimark, M. Bulow, Q. M. Wang, *Nano Letters* 2003, **3**, 713.

(S5) X. Zhou, Z. Xu, M. Zeller, A. D. Hunter, *Chem. Commun.* 2009, **36**, 5439.

(S6) S. J. Garibay, Z. Wang, S. M. Cohen, *Inorg. Chem.* 2010, **49**, 8086.

(S7) W. Morris, R. E. Taylor, C. Dybowski, O. M. Yaghi, M. A. Garcia-Garibay, *J. Mol. Struct.* 2011, **1004**, 94.

(S8) W. Morris, C. J. Doonan, O. M. Yaghi, *Inorg. Chem.* 2011, **50**, 6853.

(S9) Y. Rao, T. F. Kemp, M. Trudeau, M. E. Smith, D. M. Antonelli, *J. Am. Chem. Soc.* 2008, **130**, 15726.